Multiloop linkage dynamics via geometric methods

Multi-loop Linkage Dynamics via Geometric Methods: A Case Study on a RH200 Hydraulic Excavator

B.R.A. Janssen, M.M.J. Nievelstein

DCT.2005.40

Internship report

Supervisors: Prof. Dr. M. Steinbuch
Dr. R. McAree
Co-worker: N. Hillier

University of Queensland, Brisbane, Australia
Department of Mechanical Engineering

Eindhoven University of Technology
Department of Mechanical Engineering
Dynamics and Control Group

Eindhoven, 10 October 2003

Multiloop linkage dynamics via geometric methods

A case study on a RH200 hydraulic excavator

Stage report

University of Queensland
Faculty of Mechanical Engineering
Brisbane, Australia

14 April 2003

◄►

17 July 2003

Eindhoven, 10-10-03

Bart Janssen s459067
Mark Nievelstein s458781

Supervisors:
Dr. Ross McAree p.mcaree@uq.edu.au
Prof. Dr. ir. M. Steinbuch M.steinbuch@tue.nl

Co-workers:
Nicholas Hillier n.hillier@crcmining.com.au

Table of Contents

1. Introduction

This "stage" report is part of the result of a traineeship at the Department of Mechanical Engineering at the University of Queensland, Brisbane, Australia. From 14 April 2003 until 17 July 2003. We, Bart Janssen and Mark Nievelstein, studied the dynamics of multi-loop rigid body linkages, based on geometric methods, in general and the dynamics of the digging mechanism of an O&K RH200 hydraulic excavator in particular. During our 14-week study we've been supervised by Dr. P.R.McAree and have been working in co-operation with Nick Hillier, a UQ PhD student.

This report can be seen as an addition to the main output of our study, a preliminary paper on *"Multiloop linkage dynamics via geometric methods"*. This paper, initiated by Dr. P.R. McAree and N.Hillier, has been a starting point for our work, which has taken the paper from an idea to a complete description of a solution method for the forward dynamics of rigid body linkages containing (multiple) closed loops, based on geometric methods. The purpose of this additional report is to give an idea of what was at the origin of the paper, it's background and what work has been done that led to the paper, since the paper itself only gives a result

Figure 1.1 *O&K RH200 hydraulic excavator in operation (From "Mining Hydraulic Excavators", Terex Mining)*

1.1 Problem statement

The study on the multi body dynamics of the O&K RH200 hydraulic excavator (figure 1.1) is part of a larger project whose objective is to increase the efficiency of the machines operation. The part that is focussed on here consists of a dynamic measurement of the mass of the material in the bucket from the cylinder pressures during operation, for which a dynamic model of the digging mechanism is indispensable. The objective for the study on the dynamics of the digging mechanism in particular is to form a neat description and solution method for its forward dynamics, containing multiple closed loops, that is suitable for real-time applications in the estimation procedure of the mass of the material in the bucket.

1.2 Report structure

Chapter two covers the background of the overall project on the RH200 and the role of the dynamics of the digging mechanism in this project, on basis of which the problem statement has been refined. Chapter three comprises a summary of the work that has been done which lead to the preliminary paper. In chapter 4 there is some explanation about this paper and finally, in chapter 5 conclusions and recommendations on the overall traineeship are included. For conclusions on the multi body dynamics problem itself we refer to conclusions and recommendations in the paper.

2. Background

For several years the Department of Mechanical Engineering at the University of Queensland and the CMTE (Centre for Mining Technology and Equipment – now CRCMining) have been working on a project to increase the efficiency of digging equipment in open cut excavation mining, a common practice in Australia. As a case study they're working on an O&K RH200 hydraulic excavator because one of these machines in a pit in Western Australia can sometimes be used for experiments and data analysis.

2.1 The Machine

The machine under study is the O&K RH 200 hydraulic excavator, which is depicted in figure 1.1. It is used in open cut excavation to dig in relatively soft, or blasted material. To get an impression of the size of the machine, some technical specifications of the RH200 are given in figure 2.1. The main advantage of the use of these mobile hydraulic excavators (compared to other open cut digging equipment) is that selection of the highest quality material can be done during digging, which saves digging up and processing low quality material.

Model		RH 200
Front Shovel, Standard	m^3 SAE 2:1/1:1	26.0/30.5
Backhoe, Standard	m^3 SAE 1:1	26.0
Engine		2 x Cummins Serie 38
Output/Speed	kW (HP)/RPM	1680 - 1880 (2250 - 2520)/1800
Control /Output governing		hydr. servo/PMS
Track pad width	mm	1400/1600/1800
Undercarriage width	mm	7000 (1400)
Crawler length	mm	8545
Drawbail pull	kN	2520
Ground bearing pressure	N/cm^2	23.5 (1400)
Weight approx	t	480
Face shovel: crowd-/breakout force	kN	1890/1500
Backhoe: tearout-/breakout force	kN	1200/1200

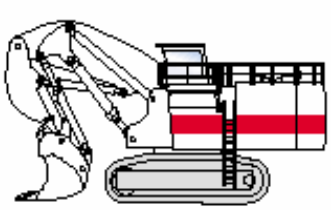

Figure 2.1 *Some technical specifications of the RH200 hydraulic excavator (From "Mining Hydraulic Excavators", Terex Mining)*

In a mining pit these machines are situated in front of a "face", an almost vertical muck pile of soft or blasted material of about 10 m high. The bucket enters this pile horizontally at the bottom. After a couple of meters the horizontal motion, "crowd", is changed into a vertical lift of the bucket along the side of the face. At the top of the face the whole upper carriage twists and the bucket position is adjusted to meet the waiting haul truck, above which the bucket is opened and the material is dumped. [31].

2.2 The digging mechanism

As one can see from figure 2.1 the digging mechanism of the RH 200 has not just a standard configuration of a bucket connected to the machine housing by a boom and a stick, where each joint is actuated by a hydraulic cylinders, but the more complex configuration with some additional links. The mechanism and the names of its links are shown clearly in figure 2.2.

The RH 200 digging mechanism is characterized by the so-called "Tripower", the triangular shaped link attached to the boom. It is claimed by the manufacturer that this digging mechanism has two main advantages over the standard configuration:

- The tilting of the bucket, actuated by the bucket cylinder, is more or less decoupled from the motion of the stick and the boom. To dig with a constant angle of the bucket with respect to the horizon, the operator only needs to operate

two (boom and stick) cylinders and not three cylinders as in the conventional situation.

- Because of a more favorable transfer ratio of forces in the mechanism, there's more "digging" force at the tip of the bucket compared to standard mechanism when operated at the same cylinder forces.

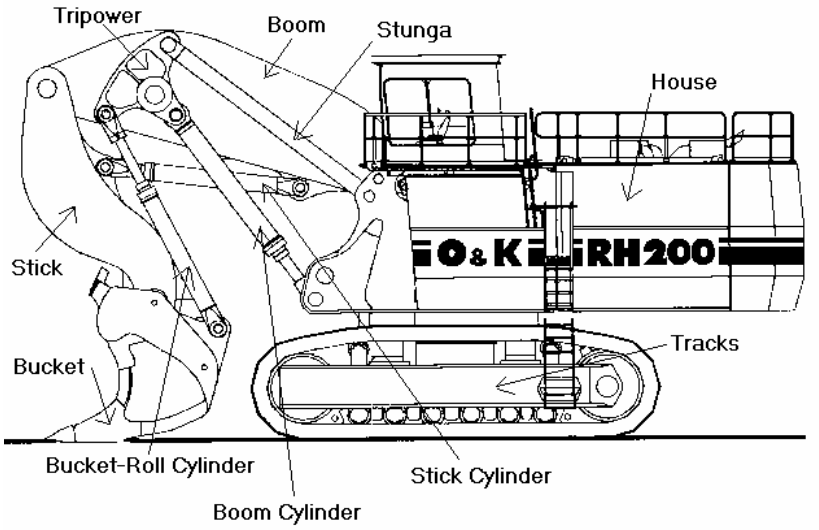

Figure 2.2 *RH 200 hydraulic excavator digging mechanism and its terminology [31]*

From a close look at the mechanism one can see that it consists of 11 links and 15 1 DOF joints (a hydraulic cylinder can be seen as two links connected by a prismatic joint), which yields a total of 3 DOF for the whole mechanism. From fig. 2.2 it can also be seen that the mechanism consists of multiple closed loops.

2.3 The project

One way that is investigated in the project to increase efficiency of the RH200 is to try to increase the bucket fill factor. One can imagine that the bucket fill factor is heavily dependent on the digging cycle of the bucket, which is controlled by the operator. Previous work on the RH200 [31] reveals that different operators achieve significantly different bucket filling factors.

To determine the optimal digging cycle, one needs to know the amount of material in the bucket each dig.

One would think this could be easily accomplished by a static measurement of the hydraulic pressures in the cylinders in a pause of the machine during a dig cycle. However, a demand from the mining company supplying the O&K RH200 for testing is, that in no way the productivity of the machine is deteriorated by experiments or data analysis. That rules out the possibility of a pause in each dig cycle for a static pressure measurement. Only a dynamic pressure measurement in the part of the digging cycle when the bucket is moving from the pile to the haul truck can reveal the mass of the material in the bucket. To calculate the mass of the material in the bucket from dynamical pressure measurements, one needs to compensate for the dynamical effect. For this compensation a dynamic model of the digging mechanism is essential.

It seems very laborious to set up a dynamic pressure measurement only to determine the mass of the material in the bucket, for which also position / velocity sensors have to be fitted on the RH200. However, in a wider scope of the work on efficiency increasing, one is also interested in automation of mining equipment, for which these types of measurements are essential. One is also interested in the relationship between machine wear and -damage and bucket fill factors, for which continuous monitoring of the mass of material in the bucket is also desirable.

2.4 Problem Statement: Multi Body Dynamics

From a dynamic measurement of the hydraulic pressure in the cylinders and measurements of position and velocity of (all) links in the digging mechanism the mass of the material in the bucket can be calculated using an extended Kalman filter, provided that there's a dynamic model of the mechanism.

The aim of this study is to derive a model for the forward dynamics of the 12-linkage digging mechanism, as in figure 2.2, which is suitable for (real-time) implementation in an extended Kalman filter, which is capable of estimating the mass of material in the bucket. On forehand the following assumptions were made to define the problem:

- The Kalman filter or actual mass- calculation is not considered
- Cylinder forces, link positions and link velocities are available from measurements. The measurements itself are not considered.
- The links in the digging mechanism are assumed to be rigid
- Only the linkage under actuation of the cylinder forces is considered, external, disturbance or other forces are neglected.

Under these assumptions the problem of modeling forward dynamics reduces purely to that of the construction of an algorithm, which, for an input of cylinder forces, link positions and link velocities, gives the link accelerations. These can then be integrated to obtain a prediction of the link positions. This algorithm should be suitable for (real-time) implementation in the calculation of the mass in the bucket. The handling of the closed loop topology of the mechanism will be the major difficulty.

3. Problem approach

In this section there will be a brief overview of how the problem of finding an appropriate algorithm to describe the forward closed loop dynamics of the digging mechanism has been approached.

3.1 Size reduction

First, to simplify the problem, the 12 bar digging mechanism was reduced to a simple closed loop 4 bar mechanism (figure 3.1)

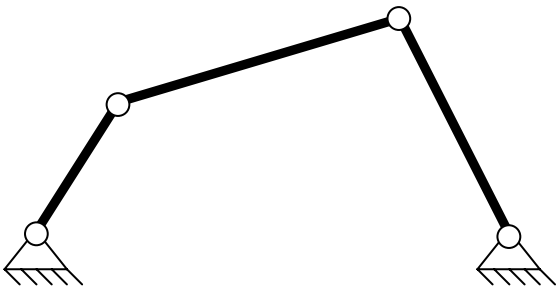

Figure 3.1 A simple closed loop 4 bar linkage

This is the simplest possible form of a closed loop linkage.

3.2 Plűcker coordinates

Adopting plűcker coordinates made another 'simplification' to the problem. The basic idea behind plűcker coordinates is that every infinitesimal motion can be described by a infinitesimal translation along a line and a infinitesimal rotation around this same line. Derivatives in plűcker coordinates can be expressed using Lie algebra. Because of this, especially for rigid body linkage dynamics, the use of plűcker coordinates yields notational simplicity. More about this is in the paper's appendix A and [24].

Since work on the problem had been initiated in plűcker coordinates by Dr. R.P. McAree and N.Hillier (which was kind of a standard at the UQ Engineering Department) we adopted the plűcker notation as well. It is also used in the literature about rigid body linkages dynamics.

3.3 DAE

The standard method to handle closed loops in a linkage is to cut the loops at designated joints, the cut joints, to create an open linkage. To ensure the dynamics of the cut mechanism match the dynamics of the closed loop system, constraints on the position of the cut joint are introduced, which result in constraint forces in the linkage dynamics.

The problem of solving the closed loop dynamics of the 4-bar linkage (or any linkage containing closed loops) then comes down to solving a differential algebraic equation (index-3 DAE). The open loop dynamics, including the constraint forces resulting from the cut, form the differential equations and the holonomic position constraints form the algebraic constraints.

The resulting closed loop dynamics of any closed loop system are in the form of a DAE of index 3. A study on numerically methods revealed that, based on present methods, index 3 DAE's are practically unsolvable directly, due to numerical instability.

Another way of handling an index 3 DAE that was considered, is reverting to a set of minimal coordinates by substituting the constraints into the differential equations, which results in one (highly non-linear) ODE for each degree of freedom of the linkage. This method was implemented for the 4-bar linkage and yielded one highly non-linear ODE in one minimal coordinate. This ODE was then solved in Matlab using different standard ODE solvers. For all solvers the result was the same:

- The solvers were slow, because of the huge highly non-linear (symbolic) ODE that had to be evaluated.
- The solution suffered significantly from numerical drift, which was of different magnitude for the different ODE solvers.

From these results we concluded that this method might be useful for a 4-bar linkage, but not for a 3 DOF 12-bar linkage which would result in an even more complex system of three ODE's.

We then adopted the classical method of calculating the Lagrange parameters from the derivatives of the holonomic position constraints and then solving the resulting ODE's with an additional stabilization step to keep the solution on the constraint manifold.

3.4 Matlab Simmechanics

In the process of solving the forward dynamics we extensively used the Matlab toolbox SimMechanics. For simulating linkage dynamics it is a very user-friendly toolbox, also for (multi) closed loop systems. In the project it was used to verify the solutions from our own algorithms.

Some effort has been put into finding the method by which SimMechanics handles closed loop topologies. A paper on Simmechanics [29] claimed to give insight in this, but it only led from one reference to the other revealing very little.

3.5 From 4-bar to 12-bar

The next step was to go from a single closed loop 4-bar mechanism (to understand some parts of the plűcker coordinate system and the problem we even started with a two link serial chain) to a multi closed loop 12-bar mechanism including translational joints. In this process, which was characterized by trial and error, every method / solution was verified using Simmechanics. The main difficulties were:

- How to use plűcker coordinates
- How do plűcker coordinates transform under motion
- How to get multi body EOM in plűcker coordinates
- Implementing recursive methods
- How to handle closed loops in general
- How to compute Lagrange parameters in plűcker coordinates
- How to handle multiple closed loops
- Choice of cut joints

Solving these difficulties one by one, each time adding links to the 4-bar mechanism, in the end resulted in complete algorithm to compute the forward dynamics of the 12-bar digging mechanism. The verification of the results from the algorithm with the Simmechanics results

on an acceleration level (disregarding the integration step) did not indicate any significant difference. (Difference of $O(10^{-12})$)

A set of Matlab m-files and Simulink files is available in which the algorithm and verification is implemented.

3.6 General Algorithm

When the algorithm for the forward dynamics of the 12-bar linkage was completed, all difficulties concerning the use of plűcker coordinates and (multiple) closed loops were overcome. This cleared the path for extension to a general method to compute the forward dynamics of (multiple) closed loop systems. That has been the focus in the last weeks of the traineeship.

The main difficulty in extending the algorithm for the 12-bar mechanism to a generalized algorithm was how to cope with any arbitrary topology. As a solution to this problem so called topology matrices have been introduced. These make it relatively easy to access information about the dependencies of links within the algorithms.

4. Preliminary Paper

Accompanying this report is the preliminary paper "Multiloop Linkage Dynamics through Geometric methods", which is the main output from the traineeship.

The paper is meant to be mainly of educational use. The concepts used in the paper are not new, only combined to result in one applicable algorithm, where much attention is paid to an example in which all difficulties concerning the handling of closed loops are implemented.

To keep the physical meaning of the equations intact the algorithm is not optimized for computational efficiency.

It should be of good use for someone having the same problem as we started with: computation of the forward dynamics of a (multi) closed loop mechanism

As stated before the paper is preliminary and not ready for submitting, but it does reflect the end result of the traineeship. The main text covering the theory and the algorithms, as it is, is considered fairly complete and finished. The main things that need more work are section 9, *Simulation \ Computational efficiency* and section 10, *Conclusions*.

However, before one can consider submitting the paper, the algorithms need to be verified. The algorithms in the paper are a generalization of the algorithm used for the 12-bar mechanism. This algorithm has been verified and proven to be correct, but the generalized algorithms are much more complicated due to the special topology matrices, introduced to handle any arbitrary system and have not been implemented yet.

5. Conclusions & Recommendation

For conclusions and recommendations on the multi-body dynamics problem itself we refer to section 10, *conclusions* of the paper. Here we will discuss the conclusions/remarks about the project.

First it should be noted that the background of the problem and it's applicability in an extended kalman filter has not been investigated or questioned, because it was considered to be outside the scope of our assignment.

5.1 Conclusions

The goal to construct a dynamic model for the 12-bar digging mechanism of the RH200 Hydraulic excavator has been achieved. The resulting model has been implemented in Matlab and has been successfully verified with SimMechanics. (A set of Matlab and Simulink files is available.) This clears the path to construct the actual estimation algorithm to estimate the mass of material in the bucket.

The model for the 12-bar linkage then was successfully extended to an algorithm for an arbitrary multi-loop multi rigid-body system, which has been the subject of the preliminary paper (initiated by Dr. R.P. McAree and N. Hillier). The paper has been finished up to a level that reflects the content of the trainee ship. It should be noted that the paper is not yet ready for submission for publication.

In contrary to other papers on closed loop linkage dynamics, the algorithm presented in this paper is very straightforward and direct applicable to closed loop linkage dynamics problems. The key features in this paper that make it preferable over other papers are:

- Use of plucker screw coordinates for a neat and clear notation.
- Use of topology matrices to handle arbitrary linkage configurations.
- Use of recursive methods, providing efficient and straightforward algorithms
- Extensive use of example(s) throughout the paper make it very applicable to any other problem.
- An appendix on basic geometric methods.

The straightforwardness and applicability of the algorithm however, comes at the cost of computational efficiency. From literature there are many methods available to increase the algorithms efficiency. For now, these have not been implemented to maintain the insight in the physical background and the equations involved.

5.2 Recommendations

Concerning the preliminary paper, the presented general algorithm, which is based on the method used to solve the 12-bar problem has, to be implemented and verified. As mentioned in section 4 of this report some sections of the paper need some improvements.

In a wider scope of the project, the dynamic measurement of the mass of the material in the bucket of the H200 excavator, the next step is to construct an estimation algorithm to perform the actual mass estimation.

When the mass measurement will actually be implemented on the machine, the computational efficiency of the dynamic model might need to be increased. From literature however, there are many methods available to increase the algorithms efficiency.

Acknowledgements

We want to thank all the people that have helped us to make our traineeship at UQ to a success, in particular:

Dr. Ross McAree	for giving us the opportunity to do our traineeship at UQ. Who has been a great supervisor and came up with new ideas each time we were stuck.
Nick Hillier	for being a great co-worker and support; who showed us around at the Engineering Department and answered many questions.
Andrew Hall	for sharing his information on the digging cycles of the RH200 and who's figures and photo's we could use.
Prof H. Gurgenci	for giving us the opportunity to do our traineeship at UQ.
Lynn Nielsen	for helping us with our visa application
Mrs. R. Clements & Mrs. V. Hutchinson	for organizing all kind of supporting facilities
Dr. ir. N v.d. Wouw Dr. ir. P.F. Lambrechts	for some good hints

University of Queensland: http://www.uq.edu.au
Technical University Eindhoven: http://www.tue.nl
Centre for Mining Technology and Equipment: http://www.cmte.org.au

References

See references in preliminary paper: "*Multiloop Linkage Dynamics via Geometric Methods*" that comes along with this report.

Multiloop linkage dynamics via geometric methods

P. R. McAree [b,a,*] M. Nievelstein [a,c] B. Janssen [a,c]

N. S. Hillier [b,a]

[a] *Division of Mechanical Engineering, University of Queensland, Brisbane, Australia, 4072.*

[b] *Cooperative Research Centre for Mining.*

[c] *Division of Mechanical Engineering, Technical University of Eindhoven, The Netherlands*

Abstract

Key words: Multi-loop linkage, geometrical dynamics, screw theory, mining equipment.

* Corresponding author.
Email addresses: p.mcaree@uq.edu.au (P. R. McAree), n.hillier@crcmining.com.au (N. S. Hillier).

1 Introduction

The equations of motion (EOMs) for systems comprised of multiple rigid bodies constrained by a closed loop topology is most readily formulated as a system of differential algebraic equations (DAEs) having the form:

$$M(\boldsymbol{\theta})\ddot{\boldsymbol{\theta}} = \boldsymbol{\tau} - \mathbf{f}(\boldsymbol{\theta}, \dot{\boldsymbol{\theta}}) - G(\boldsymbol{\theta})^T \boldsymbol{\lambda}(\boldsymbol{\theta}) \tag{1}$$

$$g\left(\boldsymbol{\theta}\right) = 0$$

where $\boldsymbol{\theta}$ is a vector of generalised coordinates describing the linkage configuration, M is a symmetric positive definite mass matrix encoding the inertial properties of the system bodies, $\boldsymbol{\tau}$ is a vector of generalised forces acting upon the linkage, $\mathbf{f}$ is a motion induced force vector, G is the constraint/freedom matrix and $\boldsymbol{\lambda}$ is the set of lagrangian multipliers giving the magnitude of the constraint forces.

The $g\left(\boldsymbol{\theta}\right) = 0$ expression is the algebraic condition restraining the motion of the mechanism to valid kinematic solutions by defining the configuration space of the linkage in terms of the generalised coordinates. $g(\boldsymbol{\theta})$ can be interpreted as a manifold in $\boldsymbol{\theta}$-space (which is usually not smooth) and $G(\boldsymbol{\theta})$ is the tangent space at some configuration $\boldsymbol{\theta}$.

This formulation of the dynamics as a DAE arises because of the inherent complexity of expressing the EOMs as an ordinary differential equation (ODE) incorporating the constraint equations $g(\boldsymbol{\theta})$.

A linkage giving rise to the formulation above (Eqn. 1) as investigated within this paper is shown in Fig. 1.

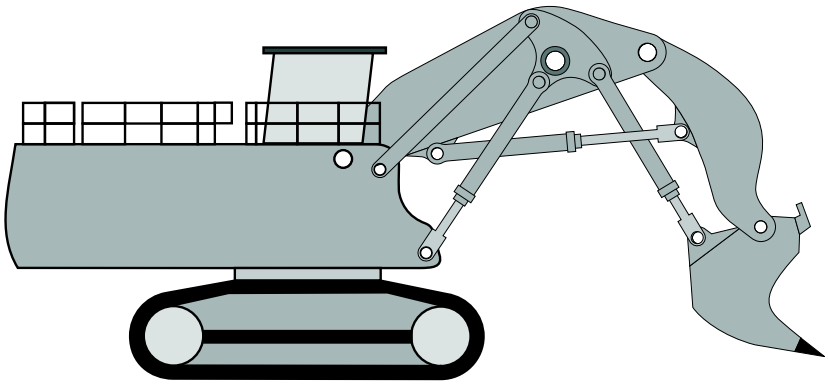

Fig. 1. **The excavation arm of a hydraulic mining excavator as an example of a mechanism having multiple kinematic loops. The arm is actuated by hydraulic cylinders providing three degrees of freedom.**

1.1 Reasons/Rationale

Some popular methods for forming the EOMs for multiple rigid-body systems are given in [2,5,11,20,22,30,29]. This paper presents a geometric formulation [17,18,24] leading to equations of the form of Eqn. 1 which offers simplicity and associated insight into the solution of the mechanism being analyzed.

This paper describes a comprehensive method for formulation of constrained multi linkage dynamics and provides applicative examples from which solutions to other problems can be formulated with appropriate changes. Some base geometric formulation theory is presented in the appendix to enable understanding of the key concepts.

1.2 Elements of the algorithm

The basic elements of the algorithm are:

- Break loops to get tree mechanisms.
- Recursively compute the link velocities.
- Construct the joint space referred mass (inertia) matrix, M, and motion induced force vector, $\mathbf{f}$.

- Construct the constraint freedom matrix, G, its time derivative (and non-explicitly, solve the magnitude of the forces of constraint at the breaks as Lagrange multipliers, $\boldsymbol{\lambda}$).
- Recursively calculate the accelerations of the links.
- Solve the resulting equations with a standard integration technique, such as Runge Kutta to solve ordinary differential equations and enforce the algebraic constraint conditions through application of a stabilization algorithm.

1.3 Studies/Brief History of closed loop linkage dynamics

Contemporary research into methods for computing the dynamics of closed loop linkages draws heavily upon earlier studies of the dynamics of open loop chains, particularly that of [1,11,12,14,21,22,26,30]. The open-loop dynamic problem is usually separated into the so-called *forward-dynamics problem*, namely that of computing the motion resulting from the application of prescribed actuator forces and the *inverse problem*, that of computing the forces required to generate a prescribed motion. Similar distinctions are equally applicable to closed loop systems.

A very early closed loop dynamic solution is presented in the work by Uicker [27] who solved the inverse dynamic problem for a single degree of freedom 7-bar linkage through the introduction of an additional degree of freedom and a relative body position-velocity-acceleration constraint on the associated new joint coordinate. Later work [28] tackled the forward dynamic problem and although a manageable method for the full analytical description of a closed loop system was developed (through application of Lagrange's method to a Denavit-Hartenburg type kinematic matrix description), the final solution was limited to a linearized subset of the full equations.

Kane and Levinson [15] reference earlier works who have handled such mechanisms through the introduction of Lagrange multipliers but are quick to point out that such methods necessitate additional terms in the formulation which

yield little insight into the problem. They move on to describe a method for the handling of systems with internal closed loops, utilizing superfluous generalized coordinates (and speeds) which are subsequently linearized. The foundation for most work by these authors are *Kane's dynamical equations* [15,16].

The primary foundation for the modern works into closed loop linkage dynamics was formed by Bae and Haug [5] who extended the examination of open loop mechanisms to closed loops through the introduction of Lagrange multipliers acting upon cut joints which then yielded an open loop mechanism. This procedure is commonly referred to as the *breaking* of the closed loops. Bae and Haug's presented formulation yields a system of index 3 DAEs [3]. Such a formulation has been generally adopted by more recent works [2,18,20,29] and that built upon here.

2 Notation

Early work in the field of multi-body rigid dynamics by Featherstone [11] introduces screw theoretic notations to his solution (combined angular and translational velocities). This notation forms a basis for geometric methods in multi-body system dynamics adopted by others, notably Selig and McAree [24,25] and Muller [18]. The solution presented here makes extensive use of the relative body Plücker coordinate representation for bodies consistent with these formulations. This allows for adaptation of the methods presented above to a much simpler and more manageable notational construct. A brief summation of these ideas has been included in the appendix.

2.1 Tree structures

Open loop mechanisms can be typified by the tree structure. Formal graph theory definitions can be found in the field of discrete mathematics [8,10] which

are equally applicable here, however, for our purposes we limit our definition to that below.

A tree structure is a multi-body system with an identifiable (and singular) root link, with one or more attached links connected through a joint and containing no closed loops. As such, there is a unique path between any two joints. The simplest example is that of a serial chain. More generally tree mechanisms take the form of Fig. 2. Fig. 1 can take many different tree forms by cutting the closed loops at different joints. Several configurations are shown in Section 8, where an example is discussed.

Leaf links: links at terminal ends of the mechanism. Leaf links have no children (see below).
Root link: link which connects to the ground or reference surface.
Levels: the root link is at level 1, all links attached to the root are at level 2, any link connected to a level 2 link (but not the root) is at level 3 and so on.
Branch: A set of links, consisting of all links directly connecting a leaf link to the root link, including the leaf and the root link
Loop's root link: The highest level link present in both branches resulting from a cut loop. In case a cut results in a multiple tree stricture or in case of a cut at a grounded joint the loop's root link is defined as the ground.

The link precedent to, or on one level below a given link, is called its parent; the direct antecedent, or one level above a link, is its child. The links above a given link i are those at levels higher than the link in question but connected to it by a sequence of joints and links, that is by the descendants of the link i. If link j is above link i we write $i \prec j$ (and vice versa for links lower than i, its ancestors).

Links should be numbered starting from the root link and numbering via levels. (see Fig. 2)

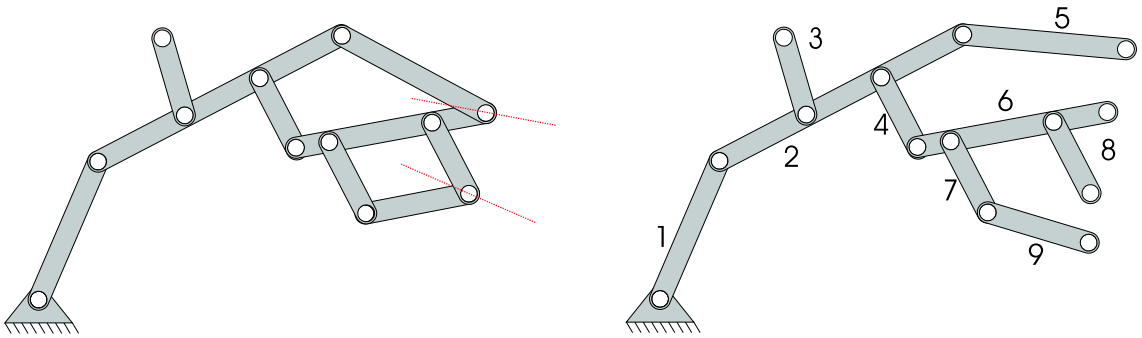

Fig. 2. **An example of a tree structure. Level 1 links: link 1. Level 2 links: link 2. Level 3 links: links 3, 4, 5. Level 4 links: link 6. Level 5 links: link 7, 8. Level 6 links: link 9. Link 1 is the mechanism's root link, links 3, 5, 8, 9 are leaf links. Link 2 is the root link of the loop formed when link 5 and 6 are connected. Links denoted by $1 \prec 8$ are links 2, 4, 6 and 8**

2.2 Topology matrices

For the purpose of formulating and calculating the dynamics in an orderly and compact way, we introduce a set of *topology matrices* to describe the topology of tree structures. This is done in preference to that of the common graph theory description of an adjacency listing [8] or an overall topology matrix. Such definitions are sufficient to describe the full mechanism topology however do not present an easy and efficient manner for access of the topology information within the algorithms.

As such we introduce matrices to handle the definition of each link's:

- parent,
- child(ren) and
- lower descendants.

Beyond this, we also require the definition of all the links participating in a loop (for each loop).

This seems very elaborate, but is convenient to access the topology information in further algorithms.

The parent information is stored in the parent vector denoted P. If link i is the root link of a tree then $P_i = 0$, otherwise, the contents of the $i-th$ element of P is the $i-th$ link's parent.

The child information is stored in the child matrix denoted C. If the $j-th$ link is a child of the $i-th$ link then $C_{ij} = j$.

The descendants information is stored in the descendants matrix denoted D. If link j is in a branch of descendants of link i (i.e. $i \prec j$), then the child of i in the branch of descendants connecting link i and j is denoted l and $D_{ij} = l$.

The loop information will be stored in the loop matrix denoted L which contains a simple reference structure for definition of a closed loop's cut joints. The number of rows in L is equal to the number of cut joints. Elements of L are ternary in value (either 1, -1 or 0). Positive or negative evaluations of a non-zero element are arbitrarily assigned upon the left and right sides of a cut joint (when viewed in a 2-D reference from an arbitrary configuration), but it suffice to say that the elements of L corresponding to joints on one side of a cut must be of opposite sign to those on the other else constraining terms from opposite sides of a cut joint will not cancel.

If joint j is part of loop i (cut by cut joint i), $L_{ij} = 1$ if the joint j is on the "left hand side" of the cut and $L_{ij} = -1$ if the joint j is on the "right hand side" of the cut. If link j is not part of loop i then the corresponding matrix element remains as initialized ($L_{ij} = 0$).

Each of the above matrices can be considered to be zero-initialized. The notation Z_{P_j} gives the quantity Z for the link denoted by element j of matrix P (and similarly for $Z_{C_{ij}}$ and the like). If the element of the subscript has a zero value, then the variable also takes on zero value (eg. if a mechanism is so numbered that link 1 has no parent, as is the norm, then $P_1 = 0$ and thus $Z_{P_1} = 0$).

3 Dynamics of tree structured mechanisms

3.1 A single rigid body

Any given rigid body subject to external forces can be written as an applied reflection of that presented by Eqn. A.21:

$$N\ddot{\mathbf{q}} + \{\dot{\mathbf{q}}, N\dot{\mathbf{q}}\} = \mathcal{F} + \mathcal{G}$$

where N is the 6 x 6 inertia matrix, $\dot{\mathbf{q}}$ is the velocity of the link and $\mathcal{G}$ and $\mathcal{F}$ are the wrenches formed from the externally acting forces due to gravity and applied forces respectively ($\mathcal{G} = N\mathbf{g}$, where $\mathbf{g}$ is the acceleration due to gravity).

If we now consider a body constrained in its motion so that it has n degrees of freedom ($n \leq 6$), distinguishing the wrenches $\mathcal{R}$ imposed by constraints from those applied externally (as above), denoted $\mathcal{F}$, and those due to gravity, denoted $\mathcal{G}$ we can write Eqn. A.21 as

$$N\ddot{\mathbf{q}} + \{\dot{\mathbf{q}},\ N\dot{\mathbf{q}}\} = \mathcal{F} + \mathcal{R} + \mathcal{G}. \tag{2}$$

Note that the constraint wrench $\mathcal{R}$ lies in the $6 - n$ dimensional space of co-screws spanning the space of constraints on the body. From the principal of virtual work (or from reciprocity), a constraint wrench can do no work on the corresponding freedom screw and it follows that (As per Eqn. A.5):

$$\mathcal{R}^T\dot{\mathbf{q}} = 0 \tag{3}$$

The dynamics of a body having n degrees of freedom can be described by a system of n scalar equations. If $\mathbf{s}_i$, $i = 1, \ldots, n$ are the screw representations of the freedoms of the body (Eqn. A.3), we can obtain these n equations from the inner product of Eqn. A.21 with the $\mathbf{s}_i$, i.e.

$$\ddot{\mathbf{q}}^T N\mathbf{s}_i + \{\dot{\mathbf{q}}, N\dot{\mathbf{q}}\}^T \mathbf{s}_i = \mathcal{F}^T\mathbf{s}_i + \mathcal{G}^T\mathbf{s}_i \quad i = 1, \ldots, n$$

which, using the identity

$$\begin{aligned} \{\dot{\mathbf{q}}, N\dot{\mathbf{q}}\}^T \mathbf{s}_i &= \dot{\mathbf{q}}^T N\, H \frac{dH^{-1}}{dt}\mathbf{s}_i \\ &= \dot{\mathbf{q}}^T N\, [\mathbf{s}_i,\, \dot{\mathbf{q}}] \end{aligned} \tag{4}$$

reduces to

$$\ddot{\mathbf{q}}^T N\mathbf{s}_i + \dot{\mathbf{q}}^T N\, [\mathbf{s}_i,\, \dot{\mathbf{q}}] - \mathcal{G}^T\mathbf{s}_i = \tau_i \quad i = 1, \ldots, n \tag{5}$$

This makes use of the interpretation of the magnitude of the component of $\mathcal{F}$ that acts directly on the freedom $\mathbf{s}_i$:

$$\mathcal{F}_i^T\mathbf{s}_i = \tau_i \tag{6}$$

An n-degree of freedom body as described by the above system of equations can also be reduced to a single (matrix) equation with $\sum_{i=1}^{n} \mathbf{s}_i = \mathbf{s}$ encoding all ($n \leq 6$) degrees of freedom for the body.

3.2 Trees - rigid bodies with joint constraints

Again, this can be expanded to the case of an open loop system (serial linkage or tree structure) by taking each freedom screw to represent the freedoms of a joint between two bodies (a joint screw). As such Eqn. A.21 for an n bodied system with each body and joint to its parent denoted by the subscript i can be rewritten as.

$$N_i\ddot{\mathbf{q}}_i + \{\dot{\mathbf{q}}_i, N_i\dot{\mathbf{q}}_i\} = \mathcal{F}_i + \mathcal{R}_i + \mathcal{G}_i - \sum_{j=C_{ik}} (\mathcal{F}_j + \mathcal{R}_j)\,, \quad k = i...n$$

where n is the total number of links.

The summation on the RHS of the above is over all j, the children of link i. The constraining wrenches (the $\mathcal{R}$ terms) are the internal reaction wrenches at the joints between intersecting bodies.

Summating over the descendants of (and including) link i in the tree ($i \preceq j$)

will cancel the reaction wrenches on the RHS of the individual link equations:

$$\sum_{j \succeq i} \left(N_j + \{ \dot{\mathbf{q}}_\mathbf{j} N \dot{\mathbf{q}}_\mathbf{j} \} - \mathcal{G}_j \right) = \mathcal{F}_i + \mathcal{R}_i \tag{7}$$

Again, taking τ_i to be the generalized force applied at joint i from Eqn. 6 and redefining Eqn. 3 as:

$$\mathcal{R}_i^T \mathbf{s}_i = 0 \tag{8}$$

allows us to multiply through by the appropriate joint screws and derive expressions for the actuating forces.

$$\sum_{j \succeq i} \left(\ddot{\mathbf{q}}_\mathbf{j}^\mathbf{T} N_j + \{ \dot{\mathbf{q}}_\mathbf{j} N \dot{\mathbf{q}}_\mathbf{j} \}^T - \mathcal{G}_j^T \right) \mathbf{s_i} = \mathcal{F}_i^T \mathbf{s_i} = \tau_i \tag{9}$$

3.3 Handling closed loop mechanisms by forming trees

The formulations above (Eqns. 7 and 9) are easily extended to provide a basis for closed-loop mechanisms with the introduction of additional constraints.

Each individual closed loop can be cut at an arbitrary joint, transforming the loop to a localised serial or tree-type structure [5]. The reaction wrenches that would normally constrain the motion of the closed loop ($\mathcal{R}_{cons}$) are equated either side of the cut, ensuring homogeneity with the closed loop structure.

Thus, we can rewrite Eqns. 7 and 9 as:

$$\sum_{j \succeq i} \left(N_j + \{ \dot{\mathbf{q}}_j, N \dot{\mathbf{q}}_j \} - \mathcal{G}_j \right) = \mathcal{F}_i + \mathcal{R}_i + \sum_{j \succeq i} \mathcal{R}_{cons\ j} \tag{10}$$

and,

$$\sum_{j \succeq i} \left(\ddot{\mathbf{q}}_\mathbf{j}^T N_j + \{ \dot{\mathbf{q}}_j, N \dot{\mathbf{q}}_j \}^T - \mathcal{G}_j^T \right) \mathbf{s}_i = \boldsymbol{\tau}_i + \left(\sum_{j \succeq i} \mathcal{R}_{cons\ j} \right)^T \mathbf{s}_i \tag{11}$$

The equations of motion for the system are given by the composition of Eqn. 11 for each link. The resulting geometric representation is of the same form as the (desired) general form:

$$M(\boldsymbol{\theta})\ddot{\boldsymbol{\theta}} = \mathbf{f}\left(\boldsymbol{\theta}, \dot{\boldsymbol{\theta}}\right) + G(\boldsymbol{\theta})^T\lambda + \boldsymbol{\tau} \tag{12}$$

in which the homogeneity with the closed loop structure is enforced through the appropriate introduction of a lagrangian multiplier, λ, to evaluate the magnitude of the constraint wrenches at the cut joints and a constraint freedom matrix ,G, giving the freedom space of the constraints.

3.4 example: a planar four-bar mechanism

As an exemplar of these concepts we first consider the four-bar linkage as shown in Fig. 4. This linkage comprises three bodies (d_1 to d_3) connected together in a serial chain with both ends grounded (the fourth link, d_4, is the ground plane) and the mechanism is constrained by the single degree of freedom (1-DOF) rotary joints to lie in the x-y plane. Since the mechanism has one degree of freedom and three bodies, it can be described by three equations of motion and two constraint equations (the Grübler equations tell us that 3 bodies $-$ 1 degree of freedom $=$ 2 constraint equations).

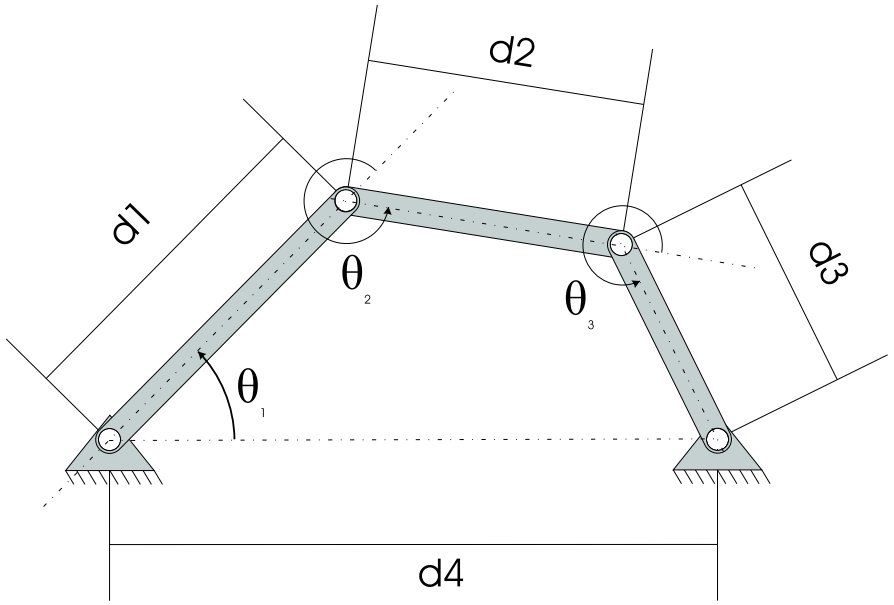

Fig. 3. **The four-bar mechanism used**

Taking Eqn. A.21 as the basis for our solution, the equations of motion for each link can be written:

$$\begin{aligned} N_1\ddot{\mathbf{q}}_1 + \{\dot{\mathbf{q}}_1,\, N_1\dot{\mathbf{q}}_1\} &= \mathcal{G}_1 + \mathcal{F}_1 + \mathcal{R}_1 - \mathcal{R}_2 \\ N_2\ddot{\mathbf{q}}_2 + \{\dot{\mathbf{q}}_2,\, N_2\dot{\mathbf{q}}_2\} &= \mathcal{G}_2 + \mathcal{R}_2 - \mathcal{R}_3 \\ N_3\ddot{\mathbf{q}}_3 + \{\dot{\mathbf{q}}_3,\, N_3\dot{\mathbf{q}}_3\} &= \mathcal{G}_3 + \mathcal{R}_3 - \mathcal{R}_4 \end{aligned} \tag{13}$$

where N_i are the inertias of the links in an inertial frame (ie. they are time variant), $\dot{\mathbf{q}}_i$ the velocities of the links in the same inertial frame, $\mathcal{R}_i$ the reaction wrench at joint i, $\mathcal{G}_i$, the wrench due to gravity acting on link i; and $\mathcal{F}_1$ the wrench acting on joint 1 (a torque of magnitude τ_1, applied at joint 1), driving the system. For this example the joint screws are (from A.12):

$$\mathbf{s}_1 = \begin{pmatrix} 0 \\ 0 \\ 1 \\ 0 \\ 0 \\ 0 \end{pmatrix}, \mathbf{s}_2 = \begin{pmatrix} 0 \\ 0 \\ 1 \\ d_1 \sin(\theta_1) \\ -d_1 \cos(\theta_1) \\ 0 \end{pmatrix}, \mathbf{s}_3 = \begin{pmatrix} 0 \\ 0 \\ 1 \\ d_1 \sin(\theta_1) + d_2 \sin(\theta_1 + \theta_2) \\ -d_1 \cos(\theta_1) - d_2 \cos(\theta_1 + \theta_2) \\ 0 \end{pmatrix}$$

The link velocities are thus given by (Eqn. A.16):

$$\dot{\mathbf{q}}_1 = \begin{pmatrix} 0 \\ 0 \\ \dot{\theta_1} \\ 0 \\ 0 \\ 0 \end{pmatrix}, \qquad \dot{\mathbf{q}}_2 = \begin{pmatrix} 0 \\ 0 \\ \dot{\theta_1} + \dot{\theta_2} \\ \dot{\theta_2} d_1 \sin(\theta_1) \\ -\dot{\theta_2} d_1 \cos(\theta_1) \\ 0 \end{pmatrix},$$

$$\dot{\mathbf{q}}_3 = \begin{pmatrix} 0 \\ 0 \\ \dot{\theta_1} + \dot{\theta_2} + \dot{\theta_3} \\ \dot{\theta_2}\left(d_1 \sin(\theta_1)\right) + \dot{\theta_3}\left(d_1 \sin(\theta_1) + d_2 \sin(\theta_1 + \theta_2)\right) \\ -\dot{\theta_2}\left(d_1 \cos(\theta_1)\right) - \dot{\theta_3}\left(d_1 \cos(\theta_1) + d_2 \cos(\theta_1 + \theta_2)\right) \\ 0 \end{pmatrix}$$

Here, the angles, θ_i, are relative angles between body i and its predecessor (parent P_i).

The applied wrench is given by (Eqn. A.4):

$$\mathcal{F}_1 = \begin{pmatrix} 0 \\ 0 \\ \tau_1 \\ 0 \\ 0 \\ 0 \end{pmatrix}$$

The inertial matrix can be formed from Eqn. A.19.

For ease of reference, from here onwards, the examples presented within this paper are restricted to a planar form. Taking the plane of reference to be x-y, the rows/columns 1, 2 and 6 of the geometric representation become redundant. This allows a reduction in the presented reference set to size 3.

The $\mathcal{R}_4$ terms on the RHS of Eqn. 13 are in effect the constraining force terms of the closed loop. The closed topology presented by the four bar mechanism prevents a straightforward computation of the forward dynamics using a tree structure. For application of this solution method, the mechanism has to be transformed into such a structure by making a *cut* at a joint (known as the *cut joint*). This will yield a binary structure with the reaction forces that act upon the cut joint ensuring the motion remains consistent with the homogenous structure (Section 5. The most convenient choice of the cut joint here would be joint 4 (or joint 1), which would result in a three link serial mechanism.

Summating the base equations above (13) according to Eqn. 10 yields:

$$\begin{aligned} \sum_{1}^{3} N_i \ddot{\mathbf{q}}_i + \{\dot{\mathbf{q}}_i, N_i \dot{\mathbf{q}}_i\} - \mathcal{G}_i &= \mathcal{F}_1 + \mathcal{R}_1 - \mathcal{R}_4 \\ \sum_{2}^{3} N_i \ddot{\mathbf{q}}_i + \{\dot{\mathbf{q}}_i, N_i \dot{\mathbf{q}}_i\} - \mathcal{G}_i &= \mathcal{R}_2 - \mathcal{R}_4 \\ N_3 \ddot{\mathbf{q}}_3 + \{\dot{\mathbf{q}}_3, N_3 \dot{\mathbf{q}}_3\} - \mathcal{G}_3 &= \mathcal{R}_3 - \mathcal{R}_4 \end{aligned} \tag{14}$$

Multiplying Eqn. 14 through by the appropriate joint screws as per Eqn. 11

to eliminate the internal reaction forces (with note to Eqn. 4, 6 and 8) gives:

$$\begin{aligned}
\sum_{1}^{3} \ddot{\mathbf{q}}_i^T N_i \mathbf{s}_1 + \dot{\mathbf{q}}_i^T N_i \left[\mathbf{s}_1, \dot{\mathbf{q}}_i\right] - \mathcal{G}_i^T \mathbf{s}_1 &= \tau_1 - \mathcal{R}_4^T \mathbf{s}_1 \\
\sum_{2}^{3} \ddot{\mathbf{q}}_i^T N_i \mathbf{s}_2 + \dot{\mathbf{q}}_i^T N_i \left[\mathbf{s}_2, \dot{\mathbf{q}}_i\right] - \mathcal{G}_i^T \mathbf{s}_2 &= -\mathcal{R}_4^T \mathbf{s}_2 \\
\ddot{\mathbf{q}}_3^T N_3 \mathbf{s}_3 + \dot{\mathbf{q}}_3^T N_3 \left[\mathbf{s}_3, \dot{\mathbf{q}}_3\right] - \mathcal{G}_3^T \mathbf{s}_3 &= -\mathcal{R}_4^T \mathbf{s}_3
\end{aligned} \tag{15}$$

The $\mathcal{R}_4$ terms on the RHS of the above are in effect the constraining force terms of the closed loop. As such this can be re-written to obtain our constrained equations of motion in accordance with Eqn. 11 as:

$$\sum_{i=j}^{3} \ddot{\mathbf{q}}_i^T N_i \mathbf{s}_j + \dot{\mathbf{q}}_i^T N_i \left[\mathbf{s}_j, \dot{\mathbf{q}}_i\right] - \mathcal{G}_i^T \mathbf{s}_j = \tau_j + \mathcal{R}_4^T \mathbf{s}_j \ , \ \ j = 1, ..., 3 \tag{16}$$

Which is of the same form as Eqn. 11 (and thus leads to Eqn. 12).

4 Recursive Calculations of $\dot{\mathbf{q}}$, $\ddot{\mathbf{q}}$, $\mathbf{f}$ and M

An efficient method to reduce the computational burden of the algorithm was shown by Walker and Orin [30] through the introduction of recursive sub-routines into the solutions. Further to this, the open loop system works [1,11,12,14,22] developed recursive calculation procedures that reduced the computational order of the problem from O(n^3) (or even O(n^4) for early works such as pointed out by Hollerbach [14]) to O(n) (where n is the number of links of the mechanism). A considerable contribution of these more efficient procedures involved the introduction of recursion into the calculation of link velocities and accelerations in the forward-dynamics problem by Featherstone [11] which saved significant computational burden and is used widely in modern works.

This section details the recursive method used to find the link velocities and accelerations, the calculation of the motion-induced force terms acting upon the links, $\mathbf{f}$, and the system mass matrix encoding the inertial properties of the

links, M. The results presented here are applicable to all open loop structures. The handling of the constraints introduced through the breaking of closed loops into open loop mechanisms is handled later (Section 5).

4.1 Recursive calculation of link velocities and accelerations

To calculate the link velocities referred to the home position (Section A.2) for a general tree mechanism, we note Eqn. A.16:

$$\dot{\mathbf{q}}_i = \sum_{1 \preceq j \preceq i} \dot{\theta}_j \mathbf{s}_j$$

and in analogy with Eqn. A.15:

$$\dot{\mathbf{q}}_i = \left(\prod_{1 \preceq j \preceq i} H_j \right) \dot{\mathbf{q}}_i^0 \tag{17}$$

Where H_k can be calculated with Eqn.A.13. Here the product $\prod_{j \preceq k \preceq l} H_k$ is the product of H_k matrices in the ancestry of link l back to and including link j (and link l). If link j is not an ancestor of link l, the product evaluates to the null matrix, except for $j = l$, when the product evaluates to identity. For notational convenience we denote:

$$\prod_{j \preceq k \preceq l} H_k = H_{j \preceq l} \tag{18}$$

for the product including link j and link l.

$$\prod_{j \prec k \preceq l} H_k = H_{j \prec l} \tag{19}$$

for the product excluding link j, but including link l.

Combining Eqn. A.16, A.15 and 17 through substitution gives:

$$\dot{\mathbf{q}}_i^0 = \sum_{1 \preceq j \preceq i} \left(H_{j \prec i} \right)^{-1} \dot{\theta}_j \mathbf{s}_j^0 \tag{20}$$

From the above expressions we can recursively compute the joint velocities referred to the home position, $\dot{\mathbf{q}}_i^0$. For a simple 2-link serial chain, Eqn. 20 can be expanded to:

$$\dot{\mathbf{q}}_2^0 = \dot{\theta}_2 \mathbf{s}_2^0 + H_2^{-1} \dot{\theta}_1 \mathbf{s}_1^0 = \dot{\theta}_2 \mathbf{s}_2^0 + H_2^{-1} \dot{\mathbf{q}}_1^0$$

For a general tree mechanism, utilizing the topological properties of the parent matrix P (Section 2.2), this is:

$$\dot{\mathbf{q}}_i^0 = \dot{\theta}_i \mathbf{s}_i^0 + H_i^{-1} \dot{\mathbf{q}}_{P_i}^0 \tag{21}$$

The acceleration of the link referred to the home position can similarly be computed through recursion.

$$\ddot{\mathbf{q}}_i^0 = \ddot{\theta}_i \mathbf{s}_i^0 + \dot{\theta}_i \left[\dot{\mathbf{q}}_i^0,\ \mathbf{s}_i^0 \right] + H_i^{-1} \ddot{\mathbf{q}}_{P_i}^0 \tag{22}$$

Now, rewriting Eqn. 22 in matrix form yields some more insight:

$$\begin{pmatrix} \ddot{\mathbf{q}}_1^0 \\ \ddot{\mathbf{q}}_2^0 \\ \vdots \\ \ddot{\mathbf{q}}_n^0 \end{pmatrix} = \begin{pmatrix} I_{6\times6} & 0_{6\times6} & 0_{6\times6} & \dots & 0_{6\times6} \\ {H_{1\prec2}}^{-1} & I_{6\times6} & 0_{6\times6} & \dots & 0_{6\times6} \\ \vdots & \vdots & \ddots & \vdots & \\ {H_{1\prec n}}^{-1} & {H_{2\prec n}}^{-1} & \dots & I_{6\times6} & \end{pmatrix} \times \left\{ \begin{pmatrix} \mathbf{s}_1^0 & \mathbf{0}_{6\times1} & \mathbf{0}_{6\times1} & \cdots & \mathbf{0}_{6\times1} \\ \mathbf{0}_{6\times1} & \mathbf{s}_2^0 & \mathbf{0}_{6\times1} & \cdots & \mathbf{0}_{6\times1} \\ \vdots & \vdots & \vdots & \ddots & \vdots \\ \mathbf{0}_{6\times1} & \mathbf{0}_{6\times1} & \mathbf{0}_{6\times1} & \cdots & \mathbf{s}_n^0 \end{pmatrix} \begin{pmatrix} \ddot{\theta}_1 \\ \ddot{\theta}_2 \\ \vdots \\ \ddot{\theta}_n \end{pmatrix} + \begin{pmatrix} \dot{\theta}_1 \left[\mathbf{q}_1^0, \mathbf{s}_1^0 \right] \\ \dot{\theta}_2 \left[\mathbf{q}_2^0, \mathbf{s}_2^0 \right] \\ \vdots \\ \dot{\theta}_n \left[\mathbf{q}_n^0, \mathbf{s}_n^0 \right] \end{pmatrix} \right\} \tag{23}$$

4.2 Motion-induced force vector $\mathbf{f}$ *and mass matrix M*

Equation. 11 can easily be simplified to give the dynamics of a generic structure undergoing free motion (no external forces). A recursive expression for this is as formed below.

We can write an expression for the wrench Q_i^0 due to the i-th link's motion, referred to the home position as:

$$\mathcal{Q}_i^0 = N_i^0 \left(\ddot{\mathbf{q}}_i^0\right) + \left\{\dot{\mathbf{q}}_i^0, N_i^0 \dot{\mathbf{q}}_i^0\right\} \tag{24}$$

Expanding this to obtain the net wrench P_i^0 acting on the i-th joint due to the motion of the connecting structure, referred to the home position gives:

$$\mathcal{P}_i^0 = Q_i^0 + H_i^{-1} \sum_{j=i}^{n} \mathcal{P}_{C_{ij}}^0 \tag{25}$$

Pairing with the i-th joint screw gives us an expression for the generalized force acting on joint i due solely to the mechanism's motion:

$$\tau_i = \left(\mathcal{P}_i^0\right)^T \mathbf{s}_i^0 \tag{26}$$

Eqns. 24, 25 and 26 form the basis for the recursive calculation of the forward dynamics of tree structures with which the actuation forces can be computed from the known joint positions and velocities.

The motion induced force vector $\mathbf{f}(\theta, \dot{\theta})$ in the geometric formulation (Eqn. 12) comprises the coriolis, centripetal and similar forcing terms as above, however does not include those due to the generalized accelerations of the link under study and as a result is very similar to the results above (Eqns. 24, 25 and 26). A recursive formulation of $\mathbf{f}(\theta, \dot{\theta})$ follows.

Using Eqn. 22, we can neglect the local link's generalized acceleration to define:

$$\boldsymbol{\xi}_i = \dot{\theta}_i \left[\dot{\mathbf{q}}_i^0,\, \mathbf{s}_i^0\right] + H_i^{-1} \boldsymbol{\xi}_{P_i} \tag{27}$$

Similarly, ignoring the local link's generalized acceleration, we get (from A.21):

$$\boldsymbol{\gamma}_i = N_i^0 \boldsymbol{\xi}_i + \left\{ \dot{\mathbf{q}}_i^0,\ N_i^0 \dot{\mathbf{q}}_i^0 \right\} \tag{28}$$

Summating the effects from all the children of link i:

$$\boldsymbol{\delta}_i = \boldsymbol{\delta}_i + \sum_{j=i}^{n} H_i^{-1} \boldsymbol{\gamma}_{C_{ij}} \tag{29}$$

results in an expression for the forces at joint i due to link i's (and its children's) motion:

$$f_i = \boldsymbol{\delta}_i^T \mathbf{s}_i^0 \tag{30}$$

For systems which are cut to give m multiple trees, the motion-induced force vector can be formed with a per-tree concatenation of terms into a larger system description.

$$\begin{bmatrix} \mathbf{f}_1 \\ \mathbf{f}_2 \\ \vdots \\ \mathbf{f}_m \end{bmatrix}$$

Similarly, expressions for the symmetric joint space referred mass matrix M can now be obtained recursively by setting velocity terms in Eqn. 22 to zero and introducing the link inertias. This yields (for the upper diagonal of M):

$$M_{ij} = \left(\mathbf{s}_i^0 \right)^T \left(\sum_{j \preceq k \preceq n} \left(H_{i \prec k}^{-T} N_k^0 \left(H_{j \prec k} \right)^{-1} \right) \right) \mathbf{s}_j^0 \qquad j \geq i \tag{31}$$

In which the i-j^{th} element of the matrix encodes the inertial relationships between the i^{th} and j^{th} links. Since M is symmetric, the lower diagonal can be obtained by a mirror operation on the upper diagonal of M. Expanding this

to matrix form would yield:

$$M = \begin{pmatrix} (\mathbf{s}_1^0)^T & \mathbf{0}_{1\times 6} & \cdots & \mathbf{0}_{1\times 6} \\ \mathbf{0}_{1\times 6} & (\mathbf{s}_2^0)^T & \cdots & \mathbf{0}_{1\times 6} \\ \vdots & \vdots & \ddots & \vdots \\ \mathbf{0}_{1\times 6} & \mathbf{0}_{1\times 6} & \cdots & (\mathbf{s}_n^0)^T \end{pmatrix} \begin{pmatrix} I_{6\times 6} & H_{1\prec 2}^{-T} & \cdots & H_{1\prec n}^{-T} \\ 0_{6\times 6} & I_{6\times 6} & \cdots & H_{2\prec n}^{-T} \\ \vdots & \vdots & \ddots & \vdots \\ 0_{6\times 6} & 0_{6\times 6} & \cdots & I_{6\times 6} \end{pmatrix}$$
$$\begin{pmatrix} N_1^0 & 0_{6\times 6} & \cdots & 0_{6\times 6} \\ 0_{6\times 6} & N_2^0 & \cdots & 0_{6\times 6} \\ \vdots & \vdots & \ddots & \vdots \\ 0_{6\times 6} & 0_{6\times 6} & \cdots & N_n^0 \end{pmatrix} \begin{pmatrix} I_{6\times 6} & 0_{6\times 6} & \cdots & 0_{6\times 6} \\ H_{1\prec 2}^{-1} & I_{6\times 6} & \cdots & 0_{6\times 6} \\ \vdots & \vdots & \ddots & \vdots \\ H_{1\prec n}^{-1} & H_{2\prec n}^{-1} & \cdots & I_{6\times 6} \end{pmatrix} \begin{pmatrix} \mathbf{s}_1^0 & \mathbf{0}_{6\times 1} & \cdots & \mathbf{0}_{6\times 1} \\ \mathbf{0}_{6\times 1} & \mathbf{s}_2^0 & \cdots & \mathbf{0}_{6\times 1} \\ \vdots & \vdots & \ddots & \vdots \\ \mathbf{0}_{6\times 1} & \mathbf{0}_{6\times 1} & \cdots & \mathbf{s}_n^0 \end{pmatrix}$$

As with the motion-induced force vector, the mass matrix for systems with m multiple trees can be formed with a per-tree concatenation of terms into a larger system description:

$$\begin{bmatrix} M_1 & & 0 \\ & M_2 & \\ & & \ddots \\ 0 & & M_m \end{bmatrix}$$

4.3 Algorithm for $\mathbf{f}$ *and* $\mathbf{M}$

Algorithm 1. Calculation of joint referred inertia matrix

Data : θ_i and $\mathbf{s}_i^0$

Result: The joint space referred mass matrix, M, and motion induced force vector, $\mathbf{f}$.

Initialization

$\dot{\mathbf{q}}_1^0 = \dot{\theta}_1 \mathbf{s}_1^0$

$\boldsymbol{\xi}_1 = \dot{\theta}_1 \left[\dot{\boldsymbol{q}}_1^0,\, \boldsymbol{s}_1^0\right] = 0$

$\boldsymbol{\gamma}_1 = \{\dot{\mathbf{q}}_1^0,\ N_1^0 \dot{\mathbf{q}}_1^0\}$

for $i = 1$ *to* n **do**

  Construct the H_i *matrices*

  $H_i = \mathrm{Ad}(e^{\theta_i \mathbf{s}_i^0})$

  $H_{i \prec i} = I$

Recurse from root to leaves

for $i = 2$ *to* n **do**

  $\dot{\mathbf{q}}_i^0 = \dot{\theta}_i \mathbf{s}_i^0 + H_i^{-1} \dot{\mathbf{q}}_{p_i}^0$

  $\boldsymbol{\xi}_i = \dot{\theta}_i \left[\dot{\mathbf{q}}_i^0,\, \mathbf{s}_i^0\right] + H_i^{-1} \boldsymbol{\xi}_{P_i}$

  $\boldsymbol{\gamma}_i = N_i^0 \boldsymbol{\xi}_i + \{\dot{\mathbf{q}}_i^0,\ N_i^0 \dot{\mathbf{q}}_i^0\}$

Recurse from leaf links to root

for $i = n$ *to* 1 **do**

  $\boldsymbol{\delta}_i = \boldsymbol{\gamma}_i$

  for $j = n$ *to* i **do**

    if $D_{ij} \neq 0$ **then**

      $H_{i \prec j} = H_{D_{ij}} H_{D_{ij} \prec j}$

    if $C_{ij} \neq 0$ **then**

      $\boldsymbol{\delta}_i = \boldsymbol{\delta}_i + H_i^{-1} \boldsymbol{\gamma}_{C_{ij}}$

    Form the mass matrix

    $M_{ij} = (\mathbf{s}_i^0)^T \left(\sum_{j \preceq k \preceq n} H_{i \prec k}^{-T} N_k^0 (H_{j \prec k})^{-1} \right) \mathbf{s}_j^0$

    $M_{ji} = M_{ij}$

  Form the i*-th element of vector* $\mathbf{f}$

  $\mathbf{f}_i = \boldsymbol{\delta}_i^T \mathbf{s}_i^0$

4.4 Re-example of 4-bar with different cuts (joint 3).

To illustrate the concepts of tree structures and introduce a problem with multiple trees as discussed above, the earlier example of a four-bar mechanism is re-examined using joint 3 as the cut joint. This choice results in two separate serial tree linkages. In this re-example the adjoint will be applied as well, for which a redefinition of the angles is necessary.

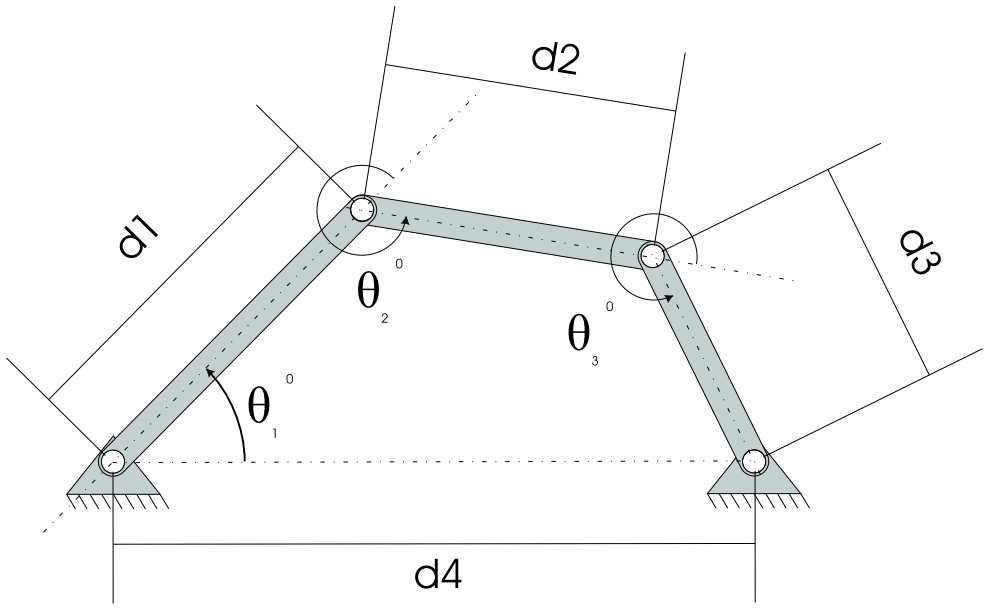

Fig. 4. **The four-bar mechanism redefined angles**

The relative angle in home position will now be denoted as $\theta_{\mathbf{i}}{}^{0}$. And $\theta_{\mathbf{i}}$ will be defined as the relative angle between two links with respect to their home position ($\theta_{\mathbf{i}}{}^{0}$). (Note that $\theta_{\mathbf{i}}$ will be 0 in home position.)

The first tree (a) consisting of links 1 and 2 based at joint 1 and the second tree (b) consisting of link 3 only, based at joint 4 (link 4 is the ground plane). According to the dissection into two trees the links will be renumbered and given an additional superscript.

$$
\begin{aligned}
{}^{a}N_1\,{}^{a}\ddot{\mathbf{q}}_1 + \{{}^{a}\dot{\mathbf{q}}_1,\, {}^{a}N_1\,{}^{a}\dot{\mathbf{q}}_1\} &= {}^{a}\mathcal{G}_1 + {}^{a}\mathcal{F}_1 + {}^{a}\mathcal{R}_1 - {}^{a}\mathcal{R}_2 \\
{}^{a}N_2\,{}^{a}\ddot{\mathbf{q}}_2 + \{{}^{a}\dot{\mathbf{q}}_2,\, {}^{a}N_2\,{}^{a}\dot{\mathbf{q}}_2\} &= {}^{a}\mathcal{G}_2 + {}^{a}\mathcal{R}_2 - {}^{a}\mathcal{R}_{cons} \\
{}^{b}N_1\,{}^{b}\ddot{\mathbf{q}}_1 + \left\{{}^{b}\dot{\mathbf{q}}_1,\, {}^{b}N_1\,{}^{b}\dot{\mathbf{q}}_1\right\} &= {}^{b}\mathcal{G}_1 + {}^{b}\mathcal{R}_1 - {}^{b}\mathcal{R}_{cons}
\end{aligned}
\tag{32}
$$

Here, ${}^{a,b}\mathcal{R}_{cons}$ refers to the constraint wrench at the cut joint and ${}^{a}\mathcal{R}_{cons} = -\,{}^{b}\mathcal{R}_{cons} = \mathcal{R}_{cons}$.

The solution proceeds by sequentially adding Eqns. 32 for each tree (as per Eqn. 10). For the first tree:

$$
\begin{aligned}
\sum_{j=1}^{2}\left({}^{a}N_j\,{}^{a}\ddot{\mathbf{q}}_j + \left\{{}^{a}\dot{\mathbf{q}}_j,\, {}^{a}N_j\,{}^{a}\dot{\mathbf{q}}_j\right\} - {}^{a}\mathcal{G}_j\right) &= {}^{a}\mathcal{F}_1 + {}^{a}\mathcal{R}_1 - \mathcal{R}_{cons} \\
{}^{a}N_2\,{}^{a}\ddot{\mathbf{q}}_2 + \{{}^{a}\dot{\mathbf{q}}_2,\, {}^{a}N_2\,{}^{a}\dot{\mathbf{q}}_2\} - {}^{a}\mathcal{G}_2 &= {}^{a}\mathcal{R}_1 - \mathcal{R}_{cons}
\end{aligned}
\tag{33}
$$

For the second tree:

$$
{}^{b}N_1\,{}^{\mathbf{b}}\ddot{\mathbf{q}}_1 + \left\{{}^{b}\dot{\mathbf{q}}_1,\, {}^{b}N_1\,{}^{b}\dot{\mathbf{q}}_1\right\} - {}^{b}\mathcal{G}_1 = {}^{b}\mathcal{R}_1 + \mathcal{R}_{cons} \tag{34}
$$

For each tree the general form of Eqns. 33, 34 is

$$
\begin{aligned}
\sum_{j=i}^{{}^{a}n}\left({}^{a}N_j\,{}^{a}\ddot{\mathbf{q}}_j + \left\{{}^{a}\dot{\mathbf{q}}_j,\, {}^{a}N_j\,{}^{a}\dot{\mathbf{q}}_j\right\} - {}^{a}\mathcal{G}_j\right) &= {}^{a}\mathcal{F}_i + {}^{a}\mathcal{R}_i - \mathcal{R}_{const} \\
\sum_{j=i}^{{}^{b}n}\left({}^{b}N_j\,{}^{b}\ddot{\mathbf{q}}_j + \left\{{}^{b}\dot{\mathbf{q}}_j,\, {}^{b}N_j\,{}^{b}\dot{\mathbf{q}}_j\right\} - {}^{b}\mathcal{G}_j\right) &= {}^{b}\mathcal{F}_i + {}^{b}\mathcal{R}_i + \mathcal{R}_{const}
\end{aligned}
\tag{35}
$$

with ${}^{a}n = 2$ and ${}^{b}n = 1$ the number of links in the tree a and b respectively.

To form equations independent of the reaction wrenches $\mathcal{R}_i$, the the inner product of Eqn. 35 is taken with $\mathbf{s}_i$ (as per Eqn. 8) to give:

$$
\begin{aligned}
\sum_{j=i}^{n_a}\left({}^{a}\ddot{\mathbf{q}}_j^{T}\,{}^{a}N_j + \left\{{}^{a}\dot{\mathbf{q}}_j,\, {}^{a}N_j\,{}^{a}\dot{\mathbf{q}}_j\right\}^{T} - {}^{a}\mathcal{G}_j^{T}\right){}^{a}\mathbf{s}_i &= \left({}^{a}\mathcal{F}_i^{T} + {}^{a}\mathcal{R}_i^{T} - {}^{a}\mathcal{R}_{cons}^{T}\right){}^{a}\mathbf{s}_i \\
\sum_{j=i}^{n_b}\left({}^{b}\ddot{\mathbf{q}}_j^{T}\,{}^{b}N_j + \left\{{}^{b}\dot{\mathbf{q}}_j,\, {}^{b}N_j\,{}^{b}\dot{\mathbf{q}}_j\right\}^{T} - {}^{b}\mathcal{G}_j^{T}\right){}^{b}\mathbf{s}_i &= \left({}^{b}\mathcal{F}_i^{T} + {}^{b}\mathcal{R}_i^{T} + {}^{b}\mathcal{R}_{cons}^{T}\right){}^{\mathbf{b}}\mathbf{s}_i
\end{aligned}
$$

Rearranging using the identity from Eqn. 4 and noting Eqn. 6 gives:

$$\sum_{j=i}^{n_a} \left({}^{\mathbf{a}}\ddot{\mathbf{q}}_j^{T\,a} N_j {}^{\mathbf{a}}\mathbf{s}_i + {}^{\mathbf{a}}\dot{\mathbf{q}}_j^{T\,a} N_j \left[{}^{\mathbf{a}}\mathbf{s}_i, {}^{\mathbf{a}}\dot{\mathbf{q}}_j \right] - {}^{a}G_j^{T}\, {}^{\mathbf{a}}\mathbf{s}_i \right) = {}^{a}\tau_i - R_{cons}^{T}\, {}^{\mathbf{a}}\mathbf{s}_i$$
$$\sum_{j=i}^{n_b} \left({}^{\mathbf{b}}\ddot{\mathbf{q}}_j^{T\,b} N_j {}^{\mathbf{b}}\mathbf{s}_i + {}^{\mathbf{b}}\dot{\mathbf{q}}_j^{T\,b} N_j \left[{}^{\mathbf{b}}\mathbf{s}_i, {}^{\mathbf{b}}\dot{\mathbf{q}}_j \right] - {}^{b}G_j^{T}\, {}^{\mathbf{b}}\mathbf{s}_i \right) = {}^{b}\tau_i + R_{cons}^{T}\, {}^{\mathbf{b}}\mathbf{s}_i$$

As before, this can be rewritten in accordance with Eqn. 11 as:

$$\sum_{j=i}^{n_a} \left({}^{\mathbf{a}}\ddot{\mathbf{q}}_j^{T\,a} N_j {}^{\mathbf{a}}\mathbf{s}_i + {}^{\mathbf{a}}\dot{\mathbf{q}}_j^{T\,a} N_j \left[{}^{\mathbf{a}}\mathbf{s}_i, {}^{\mathbf{a}}\dot{\mathbf{q}}_j \right] - {}^{a}G_j^{T}\, {}^{\mathbf{a}}\mathbf{s}_i \right) = {}^{a}\tau_i + \lambda_{ai} G_{ai}$$
$$\sum_{j=i}^{n_b} \left({}^{\mathbf{b}}\ddot{\mathbf{q}}_j^{T\,b} N_j {}^{\mathbf{b}}\mathbf{s}_i + {}^{\mathbf{b}}\dot{\mathbf{q}}_j^{T\,b} N_j \left[{}^{\mathbf{b}}\mathbf{s}_i, {}^{\mathbf{b}}\dot{\mathbf{q}}_j \right] - {}^{b}G_j^{T}\, {}^{\mathbf{b}}\mathbf{s}_i \right) = {}^{b}\tau_i + \lambda_{ai} G_{ai}$$

The above are our equations of motion according to Eqn. 11. To apply the algorithm 1 to get the system mass matrix $\mathbf{M}$ and the motion induced force vector $\mathbf{f}$ we first define the system topology matrices $\mathbf{P}, \mathbf{C}$ and $\mathbf{D}$.

$$\mathbf{P}_a = \begin{pmatrix} 0 \\ \\ 1 \end{pmatrix} \quad \mathbf{C}_a = \begin{pmatrix} 0 & 2 \\ \\ 0 & 0 \end{pmatrix} \quad \mathbf{D}_a = \begin{pmatrix} 0 & 2 \\ \\ 0 & 0 \end{pmatrix}$$

$$\mathbf{P}_b = (0) \quad \mathbf{C}_b = (0) \quad \mathbf{D}_b = (0)$$

$$\mathbf{L} = \begin{pmatrix} 1 & 1 & -1 \end{pmatrix}$$

The joint screws referred to their home position (similar to those in the previous 4-bar example) are:

$$\mathbf{s}_{a1}^{0} = \begin{pmatrix} 1 \\ \\ 0 \\ \\ 0 \end{pmatrix} \quad \mathbf{s}_{a2}^{0} = \begin{pmatrix} 1 \\ \\ d_1 \sin(\theta_1^0) \\ \\ -d_1 \cos(\theta_1^0) \end{pmatrix} \quad \mathbf{s}_{b1}^{0} = \begin{pmatrix} 1 \\ \\ 0 \\ \\ -d_4 \end{pmatrix}$$

Where $\theta^0_{a,bi}$ is the relative angle between the i-th and P_i-th link (or between the first link and the reference frame - in our case when $i = 1$) in the home position. Both the home positions for tree a and for tree b are defined at a common reference and correspond to a closed loop solution (a and b have zero relative displacement at joint 3. The coordinate frame origin is located at joint 1 of tree a as before (notice the $-d_4$ term in ${}^b\mathbf{s_1^0}$).

The transformation matrix $H_{a,bi}$ is formed from the matrix exponent of the local, relative, coordinates $\theta_{a,bi}$ with the joint screws referred to their home position (recall Eqn. A.13).

$$ {}^{a,b}H_i = Ad(e^{{}^{a,b}\boldsymbol{\theta}_i {}^{a,b}\mathbf{s}_i^0}) = e^{{}^{a,b}\theta_i {}^{a,b}\mathbf{S_i^0}} \tag{36} $$

We now can call algorithm 1 to evaluate the system mass and motion force matrices. This yields:

$$ M = \begin{pmatrix} ({}^a\mathbf{s}_1^0)^T \left({}^aN_1^0 + {}^aH_2^{-T\,a}N_2^{0\,a}H_2^{-1} \right) {}^a\mathbf{s}_1^0 & ({}^a\mathbf{s}_1^0)^T\, {}^aH_2^{-T\,a}N_2^0\, {}^a\mathbf{s}_2^0 & 0 \\ ({}^a\mathbf{s}_2^0)^T\, {}^aH_2^{-T\,a}N_2^0\, {}^a\mathbf{s}_1^0 & ({}^a\mathbf{s}_2^0)^T\, {}^aN_2^0\, {}^a\mathbf{s}_2^0 & 0 \\ 0 & 0 & \left({}^b\mathbf{s}_1^0\right)^T {}^bN_1^0\, {}^b\mathbf{s}_1^0 \end{pmatrix} $$

$$ \mathbf{f} = \begin{pmatrix} ({}^a\gamma_1 + {}^aH_1\, {}^a\gamma_2)^T\, {}^a\mathbf{s}_1^0 \\ ({}^a\gamma_2)^T\, {}^a\mathbf{s}_2^0 \\ \left({}^b\gamma_1\right)^T {}^b\mathbf{s}_1^0 \end{pmatrix} $$

where

$$
\begin{aligned}
{}^{a}\gamma_1 &= \{{}^{a}\dot{q}_1^0, {}^{a}N_1^{0a}\dot{q}_1^0\} \\
{}^{a}\gamma_2 &= {}^{a}N_2^{0a}\dot{\theta}_2\,[{}^{a}\dot{q}_2^0, {}^{a}\mathbf{s}_2^0] + \{{}^{a}\dot{q}_2^0, {}^{a}N_2^{0a}\dot{q}_2^0\} \\
{}^{b}\gamma_1 &= \left\{{}^{b}\dot{q}_1^0, {}^{b}N_1^{0b}\dot{q}_1^0\right\} \\
{}^{a}\dot{q}_1^0 &= {}^{a}\dot{\theta}_1\,{}^{a}\mathbf{s}_1^0 \\
{}^{a}\dot{q}_2^0 &= {}^{a}\dot{\theta}_2\,{}^{a}\mathbf{s}_2^0 + {}^{a}H_2^{-1a}\dot{\theta}_1\,{}^{a}\mathbf{s}_1^0 \\
{}^{b}\dot{q}_1^0 &= {}^{b}\dot{\theta}_1\,{}^{b}\mathbf{s}_1^0
\end{aligned}
$$

5 Calculation of constraint forces $G^T\lambda$

Closed loop systems, mechanisms with restricted motion or physical closed loops, are subjected to constraint. Here we only deal with position constraints, which yields holonomic constraints. The general notation for a constrained mechanical system is in the form of a third order DAE [3]:

$$
\begin{aligned}
\dot{\mathbf{q}} &= \mathbf{v} \\
M(\mathbf{q})\,\dot{\mathbf{v}} &= \mathbf{f}(\mathbf{q}, \mathbf{v}) - G(\mathbf{q})^T\lambda \\
\mathbf{g}(\mathbf{q}) &= 0
\end{aligned}
\tag{37}
$$

In which (see Eqn. 1):

- $\mathbf{q}$ are the generalized coordinates (in our case θ),
- $\mathbf{v}$ are the generalized velocities (in our case $\dot{\theta}$),
- $M(\mathbf{q})$ is the mass matrix and $\mathbf{f}(\mathbf{q}, \mathbf{v})$ contains the (non-constraining) force terms,
- $G(\mathbf{q})$ is a Jacobian of constraints defined as the derivative of the position constraint equations with respect to generalized coordinates ($\frac{\partial \mathbf{g}}{\partial \mathbf{q}}$),
- λ is a vector of lagrange multipliers and
- $\mathbf{g}(\mathbf{q})$ are the position constraint equations.

In order to solve a DAE, we can avoid numerical instability by reduction of the DAE's order. This can be accomplished by elimination of the constraints on the equation, effectively reducing the problem to an ODE bound on a manifold (reduction from an index 3 DAE to an index 1 DAE). The solution of such an ODE usually requires stabilization to ensure the solution is bound to the constraint manifold (Section 6). Elimination of the Lagrange multipliers requires the second derivative of the constraints with respect to time.

Differentiating the constraint equations $\mathbf{g}(\boldsymbol{\theta}) = 0$ with respect to t yields

$$\frac{d\mathbf{g}}{dt} = \frac{\partial \mathbf{g}}{\partial \boldsymbol{\theta}} \frac{d\boldsymbol{\theta}}{dt} = G\dot{\boldsymbol{\theta}} = 0 \tag{38}$$

A second differentiation gives

$$\frac{dG}{dt}\dot{\boldsymbol{\theta}} + G\frac{d\dot{\boldsymbol{\theta}}}{dt} = \frac{\partial G}{\partial \boldsymbol{\theta}} \frac{d\boldsymbol{\theta}}{dt}\dot{\boldsymbol{\theta}} + G\ddot{\boldsymbol{\theta}} = \frac{\partial \left(G\dot{\boldsymbol{\theta}}\right)}{\partial \boldsymbol{\theta}}\dot{\boldsymbol{\theta}} + G\ddot{\boldsymbol{\theta}} = 0 \tag{39}$$

Now we have (from 1):

$$M\left(\boldsymbol{\theta}\right)\ddot{\boldsymbol{\theta}} = f\left(\boldsymbol{\theta}, \dot{\boldsymbol{\theta}}\right) - G^T\boldsymbol{\lambda} \tag{40}$$

which can be multiplied through by GM^{-1} to give:

$$G\ddot{\boldsymbol{\theta}} = GM^{-1}f\left(\boldsymbol{\theta}, \dot{\boldsymbol{\theta}}\right) - GM^{-1}G^T\boldsymbol{\lambda}$$

substituting the acceleration constraint, $\frac{\partial \left(G\dot{\boldsymbol{\theta}}\right)}{\partial \boldsymbol{\theta}}\dot{\boldsymbol{\theta}}$, (from 39) yields:

$$-\frac{\partial \left(G\dot{\boldsymbol{\theta}}\right)}{\partial \boldsymbol{\theta}}\dot{\boldsymbol{\theta}} = GM^{-1}f\left(\boldsymbol{\theta}, \dot{\boldsymbol{\theta}}\right) - GM^{-1}G^T\boldsymbol{\lambda}$$

which can be rearranged to give the column vector of Lagrange multipliers.

$$\boldsymbol{\lambda} = \left(GM^{-1}G^T\right)^{-1}\left(GM^{-1}f\left(\boldsymbol{\theta}, \dot{\boldsymbol{\theta}}\right) + \frac{\partial \left(G\dot{\boldsymbol{\theta}}\right)}{\partial \boldsymbol{\theta}}\dot{\boldsymbol{\theta}}\right) \tag{41}$$

This can be substituted back into the equations of motion (1, 40) resulting in an ODE:

$$M\ddot{\boldsymbol{\theta}} = f\left(\boldsymbol{\theta}, \dot{\boldsymbol{\theta}}\right) - G^T\left(GM^{-1}G^T\right)^{-1}\left(GM^{-1}f\left(\boldsymbol{\theta}, \dot{\boldsymbol{\theta}}\right) + \frac{\partial \left(G\dot{\boldsymbol{\theta}}\right)}{\partial \boldsymbol{\theta}}\dot{\boldsymbol{\theta}}\right) \tag{42}$$

The process we've just gone through is called *index reduction*. We've convected a DAE of index 3 into a DAE of index 1. An interpretation of these results is that we have converted the DAE to an ODE on a manifold. The familiy of ODEs as they stand are called *un-stabilized* because they must satisfy the additional additional constraints on their states:

$$\mathbf{h} = \begin{pmatrix} g(\boldsymbol{\theta}) \\ \\ G\left(\boldsymbol{\theta}\right)\dot{\boldsymbol{\theta}} \end{pmatrix} = \mathbf{0} \tag{43}$$

5.1 Calculate $G = U^T J$

In the DAE system description (37) the $G^T\lambda$ term evaluates the constraint forces remnant from a cut joint to ensure closed loop homogeneity to the open loop structure.

As the joint screw $\mathbf{s}_i$ is the normalized basis for the motion of the joint i, the null space of $\mathbf{s}_i^T$ (denoted U_i) forms the basis for the reaction wrench at joint i. As presented earlier, the reaction wrenches do no work on the joint and as such, the product of the basis of the reaction wrench $\mathcal{R}_i$, U_i, with the velocity screw $\dot{\mathbf{q}}_i$ is zero (Eqn. 3).

The cut joint exists in two branches and as such there are two compositions for its joint screw and its transformation matrix, through each of the two branches. Both formulations are equally valid and can be used interchangeably. The cut joint's relative velocity screw ($\dot{\mathbf{q}}_i$) reflects the relative velocity of one branch with respect to the other branch resulting from the cut. This velocity can be found through subtraction of the velocities of the links previously connected by the cut joint. This relative velocity screw satisfies the principal of reciprocity Eqn. 3. (Eqn. A.16). Thus, for each cut-joint i:

$$U_i = ker\left(\mathbf{s_i^T}\right) \tag{44}$$

and

$$U_i^T \dot{\mathbf{q}} = \mathbf{0} \tag{45}$$

where:

$$\dot{\mathbf{q}}_i \;=\; \Big(L_{i1}{}^{a}\mathbf{s}_1 \; L_{i2}{}^{a}\mathbf{s}_2 \; \cdots \; L_{i{}^{a}n}{}^{a}\mathbf{s}_{{}^{a}n} \; L_{i({}^{a}n+1)}{}^{b}\mathbf{s}_1 \; L_{i({}^{a}n+2)}{}^{b}\mathbf{s}_2 \; \cdots \; L_{i\left({}^{a}n+{}^{b}n\right)}{}^{b}\mathbf{s}_{{}^{a}n} \Big) \begin{pmatrix} {}^{a}\dot{\theta}_1 \\ {}^{a}\dot{\theta}_2 \\ \vdots \\ {}^{a}\dot{\theta}_{{}^{a}n} \\ {}^{b}\dot{\theta}_1 \\ {}^{b}\dot{\theta}_2 \\ \vdots \\ {}^{b}\dot{\theta}_{{}^{b}n} \end{pmatrix} \;=\; J_i\,\dot{\boldsymbol{\theta}} \tag{46}$$

From above it can be concluded that J contains elements from all joints in the loop being cut (J consists of n columns). If the j-th joint is not in the loop being cut, the j-th column is a zero column. In accordance with the definition of $\boldsymbol{L}$, if the j-th joint is to the"left" of the cut joint, the j-th column contains the joint screw $\mathbf{s}_j$. If it is to the "right" it contains $-\mathbf{s}_j$.

Since we know from Eqn. 38 that $G_i\dot{\boldsymbol{\theta}} = 0$, and from Eqn. 45 and 46 that $U_i^T J_i \dot{\theta} = \mathbf{0}$ we can conclude for G_i:

$$G_i = U_i^T J_i \tag{47}$$

For a system containing k cut joints, the system matrix G is created by concatenating matrices for each loop, G_i, resulting in:

$$G \;=\; \Big(G_1^T \; G_2^T \; \cdots \; G_k^T \Big)^T \tag{48}$$

5.2 Time derivatives of the constraints

To solve the EOM presented in Eqn. 40, all the terms on the RHS need to be evaluated to provide a solution for the linkage accelerations. Using Eqn. 47, the acceleration constraint term in Eqn. 42, $\frac{\partial\left(G\dot{\boldsymbol{\theta}}\right)}{\partial\boldsymbol{\theta}}\dot{\boldsymbol{\theta}}$ can now be calculated

from (Recall from Eqn. 39 that: $\frac{\partial\left(G\dot{\boldsymbol{\theta}}\right)}{\partial\boldsymbol{\theta}}\dot{\boldsymbol{\theta}} = \frac{d(G_i)}{dt}\dot{\boldsymbol{\theta}}$):

$$\frac{d\left(G_i\right)}{dt}\dot{\boldsymbol{\theta}} = \left(\frac{dU_i^T}{dt}J_i + U_i^T\frac{dJ_i}{dt}\right)\dot{\boldsymbol{\theta}} \tag{49}$$

The time derivatives of U_i and J_i can be calculated with the use of the lie-bracket operand:

$$\begin{aligned}\frac{dU_i}{dt} &= ker\left(\frac{d\mathbf{s}_i^T}{dt}\right)\\ \frac{ds_i}{dt} &= \left[\dot{\mathbf{q}}_i, \mathbf{s}_i\right]\end{aligned} \tag{50}$$

and

$$\frac{dJ_i}{dt} = \left(L_{i1}\left[\dot{\mathbf{q}}_1, \mathbf{s}_1\right], \ldots, L_{in}\left[\mathbf{q}_n, \mathbf{s}_n\right]\right) \tag{51}$$

The vector $\frac{dG}{dt}\dot{\boldsymbol{\theta}}$ for a system containing k cut joints results from the concatenation of the columns $\frac{dG_i}{dt}\dot{\boldsymbol{\theta}}$:

$$\frac{d\left(G\right)}{dt}\dot{\boldsymbol{\theta}} \;=\; \left(\left(\tfrac{d(G_1)}{dt}\dot{\boldsymbol{\theta}}\right)^T \left(\tfrac{d(G_2)}{dt}\dot{\boldsymbol{\theta}}\right)^T \cdots \left(\tfrac{d(G_k)}{dt}\dot{\boldsymbol{\theta}}\right)^T\right)^T \tag{52}$$

5.3 Calculation of λ

From the basis of Eqns. 48 and 52, G and $\frac{d(G)}{dt}\dot{\boldsymbol{\theta}}$ can now be expressed as function of J_i and U_i. The Lagrange multipliers λ can now be calculated since all the terms in the RHS of Eqn. 41 are known and the EOM, in the form of the reduced DAE (Eqn. 37), can be solved for the generalized accelerations, $\ddot{\boldsymbol{\theta}}$. This results in the expression for $\ddot{\boldsymbol{\theta}}$:

$$\ddot{\theta} = M\left(\boldsymbol{\theta}\right)^{-1} f\left(\boldsymbol{\theta}, \dot{\boldsymbol{\theta}}\right) - M\left(\boldsymbol{\theta}\right)^{-1} G^T\boldsymbol{\lambda}$$

Algorithm 2. Calculation of Constraint matrix G and derivatives $\frac{d(G)}{dt}\dot{\boldsymbol{\theta}}$

Data : Matrices $H_i = \mathrm{Ad}(\theta_i \mathbf{s}_i^0)$

$\mathbf{q}_i^0$

Result: G, $\frac{d(G)}{dt}\dot{\boldsymbol{\theta}}$

For all joints (n) and cut joints (k) in the system

for $i = 1$ *to* $n + k$ **do**

Construct joint screws s_i

$\mathbf{s}_i = H_{1 \preceq i}\, \mathbf{s}_i^0$

For all cut joints in the system

for $i = 1$ *to* k **do**

Construct null space of cut-joint screw s_j

$U_i = ker\left(\mathbf{s_j^T}\right)$

Construct J_i *from*

$J_i = \begin{pmatrix} L_{i1}\mathbf{s}_1 & L_{i2}\mathbf{s}_2 & \cdots & L_{in}\mathbf{s}_n \end{pmatrix}$

Construct G_i *from*

$G_i = U_i^T J_i$

Construct $\frac{dU_i}{dt}$ *from*

$\frac{dU_i}{dt} = ker\left(\left[\dot{\mathbf{q}}_i, \mathbf{s}_i\right]^T\right)$

Construct $\frac{dJ_i}{dt}$ *from*

$\frac{dJ_i}{dt} = \begin{pmatrix} L_{i1}\left[\dot{\mathbf{q}}_1, \mathbf{s}_1\right], & \ldots, & L_{in}\left[\dot{\mathbf{q}}_n, \mathbf{s}_n\right] \end{pmatrix}$

Construct $\frac{d(G_i)}{dt}\dot{\boldsymbol{\theta}}$ *from*

$\frac{d(G_i)}{dt}\dot{\boldsymbol{\theta}} = \left(\frac{dU_i^T}{dt} J_i + U_i^T \frac{dJ_i}{dt}\right)\dot{\boldsymbol{\theta}}$

Construct G *from*

$G = \begin{pmatrix} G_1^T & G_2^T & \cdots & G_k^T \end{pmatrix}^T$

Construct $\frac{d(G)}{dt}\dot{\boldsymbol{\theta}}$ *from*

$\frac{d(G)}{dt}\dot{\boldsymbol{\theta}} = \begin{pmatrix} \left(\frac{d(G_1)}{dt}\dot{\boldsymbol{\theta}}\right)^T & \left(\frac{d(G_2)}{dt}\dot{\boldsymbol{\theta}}\right)^T & \cdots & \left(\frac{d(G_k)}{dt}\dot{\boldsymbol{\theta}}\right)^T \end{pmatrix}^T$

Again, consider the example of the four-bar cut into two tree structures (Section 4.4). To handle the closed loop topology we define the loop matrix L (Section 2.2). For the construction of L we revert to the original numbering of the four bar mechanism before the cut was made, as L describes the open-loop form of the mechanism in terms of the closed-loop form.

Thus, we have for L:

$$L = \begin{pmatrix} 1 & 1 & -1 \end{pmatrix}$$

We choose to transform the screw at the cut joint (the constrained screw) in it's home position $\boldsymbol{s}^0_{cons}$ via tree a (as opposed to via tree b - the choice is arbitrary). Using Eqn. A.15, we find $\boldsymbol{s}_{cons}$ from:

$$\mathbf{s}_{cons} = {}^{a}H_1 {}^{a}H_2 \, \mathbf{s}^0_{cons} \tag{53}$$

Which gives:

$$\mathbf{s}^0_{cons} = \begin{pmatrix} 1 \\ \\ d_1 \sin\left({}^{a}\theta^0_1\right) + d_2 \sin\left({}^{a}\theta^0_1 + {}^{a}\theta^0_2\right) \\ \\ -d_1 \cos\left({}^{a}\theta^0_1\right) - d_2 \cos\left({}^{a}\theta^0_1 + {}^{a}\theta^0_2\right) \end{pmatrix}$$

Since the wrench $\mathcal{R}_{cons}$ must satisfies $\mathcal{R}^T_{cons}\mathbf{s}_{cons} = 0$, a basis for $\mathcal{R}_{cons}$ is given by the columns u_1 and u_2 , of

$$U = \ker\left(s^T_{cons}\right)$$

The jacobian J containing the joint-screws which form the basis of the relative velocity of the cut joint is formed according to Eqn. 46.

$$J = \begin{pmatrix} {}^{a}\mathbf{s}_1 & {}^{a}\mathbf{s}_2 & -{}^{b}\mathbf{s}_1 \end{pmatrix}$$

where

$$^{a}\mathbf{s}_1 = {}^{a}\mathbf{s}_1^0$$

$$^{a}\mathbf{s}_2 = {}^{a}H_1 \; {}^{a}\mathbf{s}_2^0$$

$$^{b}\mathbf{s}_1 = {}^{b}\mathbf{s}_1^0$$

and thus

$$J = \begin{pmatrix} 1 & 1 & 1 \\ 0 & d_1 sin(^{a}\theta_1 + {}^{a}\theta_1^0) & 0 \\ 0 & -d_1 cos(^{a}\theta_1 + {}^{a}\theta_1^0) & -d_4 \end{pmatrix}$$

According to Eqn. 50 and 51 the time derivatives of U and J are then given by:

$$\frac{dU}{dt} = [\dot{\mathbf{q}}_{cons}, \mathbf{s}_{cons}]$$

and

$$\frac{dJ}{dt} = \begin{pmatrix} [^{a}\dot{\mathbf{q}}_1, {}^{a}\mathbf{s}_1] & [^{a}\dot{\mathbf{q}}_2, {}^{a}\mathbf{s}_2] & -[^{a}\dot{\mathbf{q}}_2, {}^{a}\mathbf{s}_2] \end{pmatrix}$$

where

$$^{a}\dot{\mathbf{q}}_1^0 = {}^{a}\dot{\theta}_1 \, {}^{a}\mathbf{s}_1^0$$

$$^{a}\dot{\mathbf{q}}_2^0 = {}^{a}\dot{\theta}_2 \, {}^{a}\mathbf{s}_2^0 + {}^{a}H_2^{-1} \, {}^{a}\dot{\mathbf{q}}_1^0$$

$$^{b}\dot{\mathbf{q}}_1^0 = {}^{b}\dot{\theta}_1 \, {}^{b}\mathbf{s}_1^0$$

The jacobian of the position constraints, G, can be obtained from:

$$G = U^T J$$

And its time derivative $\frac{d(G)}{dt}\dot{\boldsymbol{\theta}}$ from

$$\frac{d\,(G)}{dt}\dot{\boldsymbol{\theta}} = \left(\left(\frac{dU}{dt} \right)^T J + U^T \frac{dJ}{dt} \right) \dot{\boldsymbol{\theta}}$$

We now have computed all the necessary terms to compute λ from Eqn. 41 and can solve Eqn. 42 for the generalized accelerations $\ddot{\theta}$.

Here, the dimension of G is 2x3 and of λ, 2x1.

For the purpose of insight we present the holonomic position constraints $\mathbf{g}(\theta) = \mathbf{0}$, which define the position of the cut joint in two dimensions (the linkage planar) and form a basis for the reaction forces acting at the cut joint. In the presented method these constraints are incorporated by the kernel operation on $\mathbf{s}_{cons}$, which also provide a basis for the reaction forces acting at the cut joint.

$$\mathbf{g} = \begin{cases} d_1\cos(\theta_1) + d_2\cos(\theta_1+\theta_2) - d_3\cos(\theta_1+\theta_2+\theta_3) - d_4 = 0 \\ \\ d_1\sin(\theta_1) + d_2\sin(\theta_1+\theta_2) - d_3\sin(\theta_1+\theta_2+\theta_3) = 0 \end{cases}$$

One can check that $G = \dfrac{\partial \mathbf{g}}{\partial \boldsymbol{\theta}}$.

6 Stabilization

The solution of dynamic systems characterized by DAEs is wide and varied, but the majority suffer from instability and integral error type drift in the solutions (velocity and position drift). The most popular methods of countering the constraint violation to ensure kinematic consistency are those of Baumgarte [7] and coordinate projection [3].

Here, we integrate the EOM resultant from the index reduction of the system DAEs (Section 5) using standard 4th order Runge-Kutta integration which yields a prediction of the mechanisms' trajectory and hence a solution of the forward dynamic problem. The order reduction is based upon the second time derivative of the position constraints and as such the integration must be stabilized to conform to the position constraints. A sufficient stabilization can be achieved with a post-integral operation such as Ascher's technique [3]. The projection stabilization provides a correction of the integration step to satisfy the constraints after each integration step.

If $\hat{x}_i$ is the result of the ith integration step before the stabilization, then x_{i+1}

can be calculated with:

$$\begin{aligned} \hat{x}_i &= \begin{pmatrix} \theta_1 \ \dots \ \theta_n & \dot{\theta}_1 \ \dots \ \dot{\theta}_n \end{pmatrix}^T \\ x_i &= \hat{x}_i - F\left(\hat{x}_i\right) h\left(\hat{x}_i\right) \end{aligned} \tag{54}$$

In which $h\left(\hat{x}_i\right)$ is defined as in Eqn. 43 and $F\left(\hat{x}_i\right)$ is chosen so that the stability criterion Eqn. 55 is met.

$$\| I - H\left(\hat{x}_i\right) F\left(\hat{x}_i\right) \| \leq \rho < 1 \tag{55}$$

where:

$$H\left(\hat{x}_i\right) = \frac{dh\left(x\right)}{dx} = \begin{pmatrix} G & 0 \\ \frac{d\left(G\dot{\theta}\right)}{d\theta} & G \end{pmatrix} \tag{56}$$

where ρ is a parameter that has the same order as the integration step size. This leaves several possible choices for F [3]. The obvious choice would be $F = H^T\left(HH^T\right)^{-1}$ which satisfies Eqn. 55, but requires the expensive calculation of a large matrix inverse. Another possible choice of F would be $F = B(GB)^{-1}$ with $B = M^{-1}G^T$, which is much less expensive since the term $(GB)^{-1}$ has already been calculated in order to calculate the lagrange multipliers. However, this choice doesn't satisfy Eqn. 55, since $HF \neq I$:

$$HF = \begin{pmatrix} I & 0 \\ L & I \end{pmatrix}, \quad L = \frac{d\left(G\dot{\theta}\right)}{d\theta} B\left(GB\right) \tag{57}$$

However, if we apply this stabilization twice we get $(I - HF)^2 = 0$ which satisfies the condition that the stabilization procedure is stable itself. Moreover, this double stabilization step is still more efficient than a single stabilization step with $F = H^T\left(HH^T\right)^{-1}$. As the stabilization is applied after each step the constraints will be satisfied most accurately with minor integration step sizes.

Algorithm 3. Stabilization of the integration

Data : $K(\boldsymbol{x})$, $\hat{\boldsymbol{x}}_{i+1}$ and F($\boldsymbol{x}$)
Result: $\boldsymbol{x}_{i+1}$
for *each integration step* **do**
  apply first stabilization step
  $\hat{\tilde{\boldsymbol{x}}}_{\boldsymbol{i+1}} = \hat{\boldsymbol{x}}_{i+1} - F(\hat{\boldsymbol{x}}_{i+1})K(\hat{\boldsymbol{x}}_{i+1})$
  apply second stabilization step
  $\boldsymbol{x}_{\boldsymbol{i+1}} = \hat{\tilde{\boldsymbol{x}}}_{i+1} - F(\hat{\tilde{\boldsymbol{x}}}_{i+1})K(\hat{\tilde{\boldsymbol{x}}}_{i+1})$

7 Overall algorithm

Algorithm 4. Overall Algorithm

Data : Initial positions and velocities (state $\mathbf{x} = \begin{bmatrix} \boldsymbol{\theta}_k \\ \dot{\boldsymbol{\theta}}_k \end{bmatrix}$)

Result: Prediction of θ based on dynamic model

for *ever* **do**

read $\boldsymbol{\tau}_k$

for $j = 1$ *to number of trees* t **do**

Call Algorithm 1 to get matrix M_j *and velocity dependant force terms* $\mathbf{f}_j$ *for each tree*

Form the system mass matrix M *and velocity dependant force vector* $\mathbf{f}$ *from*

$$M = \begin{pmatrix} M_1 & 0 & 0 \\ 0 & \ddots & 0 \\ 0 & 0 & M_t \end{pmatrix} \qquad \mathbf{f} = \begin{pmatrix} \mathbf{f}_1 \\ \vdots \\ \mathbf{f}_t \end{pmatrix}$$

Call Algorithm 2 to compute G *and* $\dfrac{dG}{dt}$.

Compute the Lagrange multipliers $\boldsymbol{\lambda}$ *from*

$$\lambda = \left(GM^{-1}G^T\right)^{-1}\left[GM\left(\tau - \mathbf{f}\right) + \frac{dG}{dt}\dot{\theta}\right]$$

Compute joint accelerations from

$$\ddot{\theta} = M^{-1}\left(\tau - \mathbf{f} - G^T\lambda\right)$$

Apply Runge-Kutta integration to get $\mathbf{x}_{k+1}$

Stabilize the solution using Algorithm 3

8 12-bar exemplar

To illustrate the applicability of the method presented here to a non-trivial system, we derive the dynamics for the 12 bar linkage of a RH200 hydraulic excavator. This is a real life problem that had to be solved as part of an automation project for the machine. The main difference between the 4 and

12 bar problems is that the 12 bar mechanism has multiple, coupled loops and translational as well as rotational joints. As the remainder of the forward dynamic solution identical to that of the 4-bar linkage, we shall restrict our discussion to the handling of prismatic joints and the multiple closed loop topology.

The hydraulic cylinders are each modelled by two links connected by a prismatic joint. A prismatic joint is defined by its translational axis. Applying Eqn. A.12 to a (planar, x-y) prismatic joint gives:

$$\mathbf{s}^0 = \frac{1}{\sqrt{dx^2 + dy^2}} \begin{pmatrix} 0 \\ dx \\ dy \end{pmatrix} \tag{58}$$

To enable calculation of the mechanism's forward dynamics, the system's closed loops must be cut to form one or more tree structures. The choice of the cut joints affects the sparsity of the resulting system mass matrix and thus the numerical effort needed to solve the problem (primarily due to the inversion of the mass matrix). Here we discuss three possible configurations, resulting from three different choices of a set of cut joints.

A configuration based on the minimum number of trees is presented in Fig. 5, based on serial trees only in Fig. 6 and upon a minimal tree length form in fig. 7.

The topology matrices for configuration 1 (Fig. 5) would be:

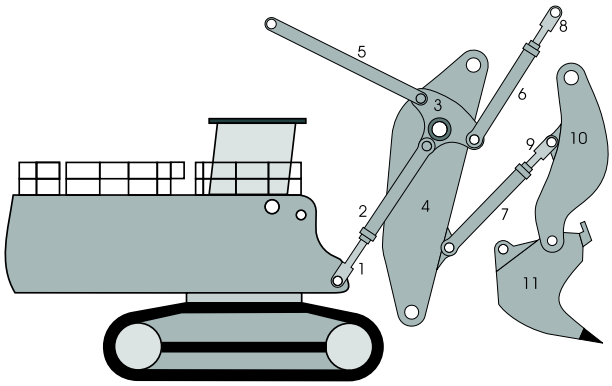

Fig. 5. **Configuration 1: Minimum number of trees**

$$P = \begin{pmatrix} 0 \\ 1 \\ 2 \\ 3 \\ 3 \\ 3 \\ 4 \\ 6 \\ 7 \\ 9 \\ 10 \end{pmatrix} \quad C = \begin{pmatrix} 0 & 2 & 0 & 0 & 0 & 0 & 0 & 0 & 0 & 0 & 0 \\ 0 & 0 & 3 & 0 & 0 & 0 & 0 & 0 & 0 & 0 & 0 \\ 0 & 0 & 0 & 4 & 5 & 6 & 0 & 0 & 0 & 0 & 0 \\ 0 & 0 & 0 & 0 & 0 & 0 & 7 & 0 & 0 & 0 & 0 \\ 0 & 0 & 0 & 0 & 0 & 0 & 0 & 0 & 0 & 0 & 0 \\ 0 & 0 & 0 & 0 & 0 & 0 & 0 & 8 & 0 & 0 & 0 \\ 0 & 0 & 0 & 0 & 0 & 0 & 0 & 0 & 9 & 0 & 0 \\ 0 & 0 & 0 & 0 & 0 & 0 & 0 & 0 & 0 & 0 & 0 \\ 0 & 0 & 0 & 0 & 0 & 0 & 0 & 0 & 0 & 10 & 0 \\ 0 & 0 & 0 & 0 & 0 & 0 & 0 & 0 & 0 & 0 & 11 \\ 0 & 0 & 0 & 0 & 0 & 0 & 0 & 0 & 0 & 0 & 0 \end{pmatrix} \quad D = \begin{pmatrix} 0 & 2 & 2 & 2 & 2 & 2 & 2 & 2 & 2 & 2 & 2 \\ 0 & 0 & 3 & 3 & 3 & 3 & 3 & 3 & 3 & 3 & 3 \\ 0 & 0 & 0 & 4 & 5 & 6 & 4 & 6 & 4 & 4 & 4 \\ 0 & 0 & 0 & 0 & 0 & 0 & 7 & 0 & 7 & 7 & 7 \\ 0 & 0 & 0 & 0 & 0 & 0 & 0 & 0 & 0 & 0 & 0 \\ 0 & 0 & 0 & 0 & 0 & 0 & 0 & 8 & 0 & 0 & 0 \\ 0 & 0 & 0 & 0 & 0 & 0 & 0 & 0 & 9 & 9 & 9 \\ 0 & 0 & 0 & 0 & 0 & 0 & 0 & 0 & 0 & 0 & 0 \\ 0 & 0 & 0 & 0 & 0 & 0 & 0 & 0 & 0 & 10 & 10 \\ 0 & 0 & 0 & 0 & 0 & 0 & 0 & 0 & 0 & 0 & 11 \\ 0 & 0 & 0 & 0 & 0 & 0 & 0 & 0 & 0 & 0 & 0 \end{pmatrix}$$

And the system's loop matrix:

$$L = \begin{pmatrix} 1 & 1 & 1 & 0 & 1 & 0 & 0 & 0 & 0 & 0 & 0 \\ 1 & 1 & 1 & 1 & 0 & 0 & 0 & 0 & 0 & 0 & 0 \\ 0 & 0 & 0 & 0 & 0 & 0 & 1 & 0 & 1 & 1 & 0 \\ 0 & 0 & 0 & 1 & 0 & -1 & 1 & -1 & 1 & 1 & 1 \end{pmatrix}$$

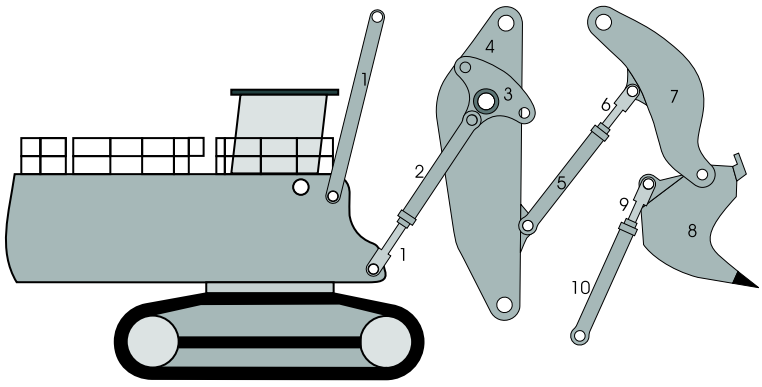

Fig. 6. **Configuration 2: Serial trees only**

The topology matrices for configuration 2 (Fig. 6) would be:

Tree a:

$$ {}^{a}P = \begin{pmatrix} 0 \\ 1 \\ 2 \\ 3 \\ 4 \\ 5 \\ 6 \\ 7 \\ 8 \\ 9 \end{pmatrix} {}^{a}C = \begin{pmatrix} 0 & 2 & 0 & 0 & 0 & 0 & 0 & 0 & 0 & 0 \\ 0 & 0 & 3 & 0 & 0 & 0 & 0 & 0 & 0 & 0 \\ 0 & 0 & 0 & 4 & 0 & 0 & 0 & 0 & 0 & 0 \\ 0 & 0 & 0 & 0 & 5 & 0 & 0 & 0 & 0 & 0 \\ 0 & 0 & 0 & 0 & 0 & 6 & 0 & 0 & 0 & 0 \\ 0 & 0 & 0 & 0 & 0 & 0 & 7 & 0 & 0 & 0 \\ 0 & 0 & 0 & 0 & 0 & 0 & 0 & 8 & 0 & 0 \\ 0 & 0 & 0 & 0 & 0 & 0 & 0 & 0 & 9 & 0 \\ 0 & 0 & 0 & 0 & 0 & 0 & 0 & 0 & 0 & 10 \\ 0 & 0 & 0 & 0 & 0 & 0 & 0 & 0 & 0 & 0 \end{pmatrix} {}^{a}D = \begin{pmatrix} 0 & 2 & 2 & 2 & 2 & 2 & 2 & 2 & 2 & 2 \\ 0 & 0 & 3 & 3 & 3 & 3 & 3 & 3 & 3 & 3 \\ 0 & 0 & 0 & 4 & 4 & 4 & 4 & 4 & 4 & 4 \\ 0 & 0 & 0 & 0 & 5 & 5 & 5 & 5 & 5 & 5 \\ 0 & 0 & 0 & 0 & 0 & 6 & 6 & 6 & 6 & 6 \\ 0 & 0 & 0 & 0 & 0 & 0 & 7 & 7 & 7 & 7 \\ 0 & 0 & 0 & 0 & 0 & 0 & 0 & 8 & 8 & 8 \\ 0 & 0 & 0 & 0 & 0 & 0 & 0 & 0 & 9 & 9 \\ 0 & 0 & 0 & 0 & 0 & 0 & 0 & 0 & 0 & 10 \\ 0 & 0 & 0 & 0 & 0 & 0 & 0 & 0 & 0 & 0 \end{pmatrix} $$

Tree b:

$$ {}^{b}P = \begin{pmatrix} 0 \end{pmatrix} \quad {}^{b}C = \begin{pmatrix} 0 \end{pmatrix} \quad {}^{b}D = \begin{pmatrix} 0 \end{pmatrix} $$

And the system's loop matrix:

$$ L = \begin{pmatrix} 1 & 1 & 1 & 0 & 0 & 0 & 0 & 0 & 0 & 0 & -1 \\ 1 & 1 & 1 & 1 & 0 & 0 & 0 & 0 & 0 & 0 & 0 \\ 0 & 0 & 0 & 0 & 1 & 1 & 1 & 0 & 0 & 0 & 0 \\ 0 & 0 & 0 & 1 & 1 & 1 & 1 & 1 & 1 & 1 & 0 \end{pmatrix} $$

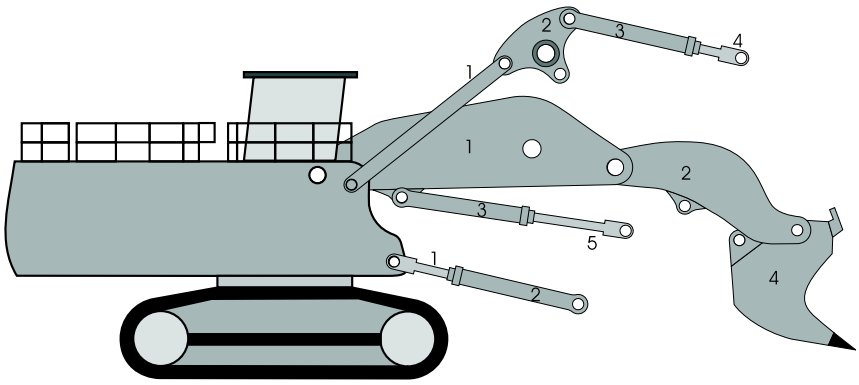

Fig. 7. **Configuration 3: Minimal tree length**

The topology matrices for configuration 3 (Fig. 7) would be:

Tree a:

$$ {}^{a}P = \begin{pmatrix} 0 \\ 1 \\ 2 \\ 3 \end{pmatrix} {}^{a}C = \begin{pmatrix} 0 & 2 & 0 & 0 \\ 0 & 0 & 3 & 0 \\ 0 & 0 & 0 & 4 \\ 0 & 0 & 0 & 0 \end{pmatrix} {}^{a}D = \begin{pmatrix} 0 & 2 & 2 & 2 \\ 0 & 0 & 3 & 3 \\ 0 & 0 & 0 & 4 \\ 0 & 0 & 0 & 0 \end{pmatrix} $$

Tree b:

$$ {}^{b}P = \begin{pmatrix} 0 \\ 1 \\ 1 \\ 2 \\ 3 \end{pmatrix} {}^{b}C = \begin{pmatrix} 0 & 2 & 3 & 0 & 0 \\ 0 & 0 & 0 & 4 & 0 \\ 0 & 0 & 0 & 0 & 5 \\ 0 & 0 & 0 & 0 & 0 \\ 0 & 0 & 0 & 0 & 0 \end{pmatrix} {}^{b}D = \begin{pmatrix} 0 & 2 & 3 & 2 & 3 \\ 0 & 0 & 0 & 4 & 0 \\ 0 & 0 & 0 & 0 & 5 \\ 0 & 0 & 0 & 0 & 0 \end{pmatrix} $$

Tree c:

$$ {}^{c}P = \begin{pmatrix} 0 \\ 1 \end{pmatrix} {}^{c}C = \begin{pmatrix} 0 & 2 \\ 0 & 0 \end{pmatrix} {}^{c}D = \begin{pmatrix} 0 & 2 \\ 0 & 0 \end{pmatrix} $$

And the system's loop matrix:

$$ L = \begin{pmatrix} 1 & 1 & 0 & 0 & 0 & 0 & 0 & 0 & 0 & -1 & -1 \\ 1 & 1 & 0 & 0 & -1 & 0 & 0 & 0 & 0 & 0 & 0 \\ 0 & 0 & 0 & 0 & 0 & 1 & -1 & 0 & -1 & 0 & 0 \\ 1 & 1 & 1 & 1 & -1 & -1 & 0 & -1 & 0 & 0 & 0 \end{pmatrix} $$

From this we can see that the topology matrices for serial linkages are of a very simple form and can easily be replaced by a loop in an automated algorithm. For a general case, as presented by configurations 2 and 3, these matrices are necessary.

9 Simulations / Computation time

The mechanism has been simulated in Matlab SimMechanics. The simulation data are used as a reference to verify the results of the calculation of the forward dynamics. The digging mechanism in home position is shown in Fig. 8

The presented algorithm has not been optimised for computational efficiency, rather it uses a geometrical notation and provides a means for substantial insight into the problem through a manageable notation. The user is able to formulate the governing equations with a minimum of effort and without resorting to numerical handling until a solution to these equations is sought.

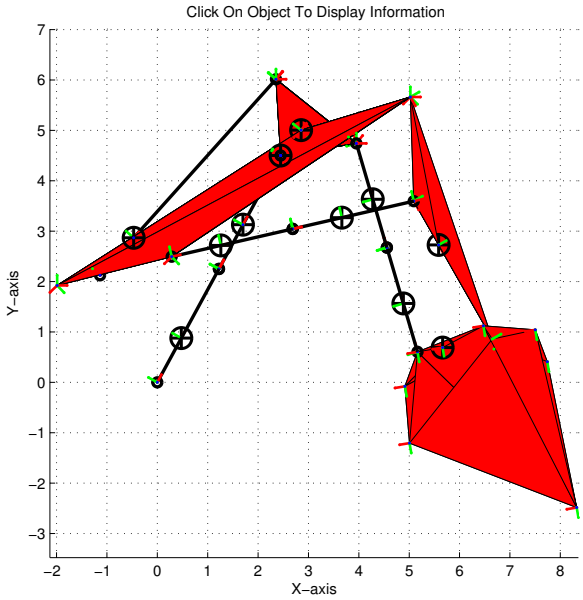

Fig. 8. **The excavation arm of a hydraulic mining excavator as in home position**

The computed solutions are highly amenable to methods that use state-space forms (eg. Kalman-Bucy filtering techniques).

The numerical efficiency of the computation method used here is of $O(n^3)$ (computation of the inverse of the system's mass matrix to solve for $\ddot{\theta}$ is an $O(n^3)$ operation). There are methods available which need less computational effort ($O(n+m)$, [2]) by introducing more recursions into the algorithm and reformulating such that the inverse of the mass matrix does not have to be computed, but rather the inverse of a replacement matrix, with dimension equal to the number of constraints. Which results in an $O(m^3)$ operation.

Examining the case of the 12 bar example here, application of an $O(n+m)$ algorithm would have unlikely led to a significant increase in the computational efficiency of the simulation (the claimed break-even point with respect to the computational costs of an $O(n+m)$ algorithm is around 12 links).

To verify the algorithms presented here only configuration 2 was simulated and compared to the simulation results from Matlab SimMechanics.
As stated above, the efficiency of the computation is affected by the choice

of the cut joints. Cutting the mechanism in to an 10 bar serial linkage and a 1 bar serial linkage will result in sub-mass matrices of 10x10 and 1x1. If the linkage is cut in one 4 bar serial mechanism one 2 bar serial linkage and one 5 bar tree linkage, the sub- mass matrices will be of size 4x4,2x2 and 5x5 respectively. The total system matrix of concatenated sub- mass matrices for the last configuration will be much more sparse then the system mass matrix for the configuration consisting of a 10 and 1 bar serial linkage. The calculation of the mass matrix will be most efficient for a configuration consisting of the maximum number of trees with minimum length.

10 Conclusion(s)

This paper presents a comprehensive method to calculate the forward dynamics of any arbitrary multi-body linkage containing closed loops (including coupled loops). From known link positions, relative link velocities and actuation forces, the link accelerations are first computed, then integrated to yield a prediction of the linkage trajectory. The main steps involved are:

- Creating an open loop tree structure by cutting the joints at specific cut joints and defining the resulting topology by topology matrices
- Calculate the transformation matrices H_i to describe the mechanisms motion and from there calculate the link velocities $\dot{\mathbf{q}}$.
- Construct the systems overall mass matrix M and overall motion induced force vector $\mathbf{f}$.
- Calculate the lagrange parameters $\boldsymbol{\lambda}$ on basis of the derivatives of the constraints
- Calculate the generalized link accelerations from $\ddot{\boldsymbol{\theta}} = M^{-1}\left(\boldsymbol{\tau} - \mathbf{f} - G^T\boldsymbol{\lambda}\right)$.
- Integrate the generalized accelerations using a stabilized integration scheme to obtain a prediction of the mechanisms trajectory.

The resulting overall algorithm heavily builds upon three parts:

- geometric methods [24], the use of plücker coordinates to define joint screws and the resulting Lie algebra yield notational ease and preserve the physical background of the equations allowing insight into the problem formulation
- recursive methods, providing efficient, straightforward algorithms
- topology matrices, which yield a concise mathematical formulation for the algorithmic description for an arbitrary mechanism. They also provide insight into the structure of the mechanism.

Other papers on forward closed loop dynamics [3,5,2,20] focus primarily on improving the efficiency of the algorithms and result in less workable methods in the absence of clear examples covering the full set of difficulties that may be encountered. This paper attempts to present a shorthand manual for one method of the calculation of forward closed loop dynamics. In contrary to other papers on forward closed loop dynamics, as mentioned above, this paper intends to be a stand-alone, applicative example suitable for direct use in forward linkage dynamics problems. The authors believe this has been achieved by a very straightforward algorithm based upon geometric methods and topology matrices as discussed above. The implementation of all steps of this algorithm is covered in detail in the examples of a 4-bar and a 12-bar multi-closed loop linkage. The basic theory on geometric methods is covered in the appendix.

The applicability and practicality of the presented algorithm and the non-recursive calculation of the inverse of the mass matrix come at the cost of computational efficiency. As presented previously, to maintain the physical insight of the equations involved, the algorithm has not been computationally optimized. The presented method is of $O(n^3)$ due to the inversion of the mass matrix that is required to calculate $\ddot{\boldsymbol{\theta}}$.

There are multiple avenues that may be pursued to optimize the algorithm. Using methods from [20] it should be possible to reduce the order of the problem to $O(m^3)$, where m is the number of constraints. This however doesn't lead to any significant numerical increase in efficiency for the problem of pri-

mary interest to the authors, that of the digging mechanism dynamics, as the number of links n (12) is of the same order as the number of constraints m (8) [2]. If methods from [2] are implemented it should, in theory, be possible to reduce the order of the problem to $\mathrm{O}(m+n)$, though this will most definitely result in a loss of insight to the physical background of the formula's involved and increase the difficulty in the problem construction.

Overall we can conclude that, considering the problem of the forward dynamics of linkages containing (multiple) closed loops, there are some very efficient algorithms available [2]. These are very useful in computational applications. The physical insights and notational forms of these methods are very limiting however. The presented method here is not optimized for efficiency, but preserves the physical background of the equations involved. For that reason and because it is presented in a applicable way, it is very workable and can be of direct use in forward dynamics problems on closed loop linkages.

A appendix

This section develops background material and notation underpinning the geometrical description of rigid body dynamics needed for the work of this paper. For comprehensive accounts of these ideas see Refs. [13,17,18,24,25]. The notation used is primarily that of Selig.

A.1 Rigid body motion; twists and wrenches; the Lie bracket

The geometrical description of rigid body dynamics draws on the Lie group structure of the group of rigid-body displacements, $SE(3)$. The spatial velocity of a body is represented by a 6-vector which is a concatenation of $\boldsymbol{\omega}$ and $\mathbf{v}$. $\boldsymbol{\omega}$ is the body's rotational velocity with respect to the global reference frame : $(\boldsymbol{\omega}_x \ \boldsymbol{\omega}_y \ \boldsymbol{\omega}_z)^T$, and $\mathbf{v}$ is the body's translational velocity in plücker coordinates,

which is given by

$$\mathbf{v} = \mathbf{w} + \mathbf{r} \times \boldsymbol{\omega} \tag{A.1}$$

in which $\mathbf{w}$ is the body's velocity in cartesian coordinates: $(\mathbf{w}_x \ \ \mathbf{w}_y \ \ \mathbf{w}_z)^T$ and $\mathbf{r}$ is the body's position vector in cartesian coordinates. Concatenating $\boldsymbol{\omega_k}$ and $\mathbf{v_k}$ into a 6-vector gives the Plücker coordinate representation of elements of $SE(3)$, Refs. [13,24]:

$$\dot{\mathbf{q}}_k = \begin{pmatrix} \boldsymbol{\omega}_k \\ \\ \mathbf{v}_k \end{pmatrix}. \tag{A.2}$$

A general infinitesimal motion corresponds to a simultaneous rotation about some axis in space together with a translation along that axis and is called a *twist*, see Refs. [6,13]. The axis about which an infinitesimal motion takes place together with the pitch of that motion (the ratio of linear to angular velocity) is called a *screw*, see Ref. [6,13]. We can obtain the screw $\mathbf{s}$ that underlies a given twist $\dot{\mathbf{q}}$ by normalizing the twist by its amplitude $|\boldsymbol{\omega}|$, i.e.

$$\mathbf{s} = \frac{1}{|\boldsymbol{\omega}|}\dot{\mathbf{q}} = \begin{pmatrix} \boldsymbol{\omega}/\left|\boldsymbol{\omega}\right| \\ \\ \mathbf{v}/\left|\boldsymbol{\omega}\right| \end{pmatrix} \tag{A.3}$$

If $\dot{\mathbf{q}}$ is a pure translation, $|\boldsymbol{\omega}| = \mathbf{0}$, and it is usual then to normalize $\dot{\mathbf{q}}$ by $|\mathbf{v}|$. Screws are geometrical elements that serve as vehicles for describing infinitesimal motion. *Inter alia*, they also provide a concise representation of the lower kinematic pairs, see Refs. [13,9,24].

The same geometrical structure, namely a spatial axis to which is associated a scalar parameter called the pitch, serves as the vehicle to describe generalized forces, see Ref. [6,13]. Specifically, any arbitrary combination of forces acting on a body can be resolved to a couple $\boldsymbol{\tau}$ acting about some line in space and a net force $\mathbf{f}$ acting along that line. This couple-force combination is known

as a *wrench*, see Refs. [6,13], and is written as a 6-vector

$$\mathcal{W} = \begin{pmatrix} \boldsymbol{\tau} \\ \\ \mathbf{f} \end{pmatrix}. \tag{A.4}$$

The rate at which the wrench $\mathcal{W}$ does work on a body twisting about $\dot{\mathbf{q}}$ is given by

$$\mathcal{W}^T\dot{\mathbf{q}} = \begin{pmatrix} \boldsymbol{\tau}^T & \mathbf{f}^T \end{pmatrix} \begin{pmatrix} \boldsymbol{\omega} \\ \\ \mathbf{v} \end{pmatrix} = \boldsymbol{\tau}^T\boldsymbol{\omega} + \mathbf{f}^T\mathbf{v}. \tag{A.5}$$

Where the wrench can do no instantaneous work, that is, where Eqn. A.5 evaluates to zero, the wrench and the twist are said to be *reciprocal*, see Ref. [13]. If $\dot{\mathbf{q}}$ is normalized to give the underlying screw, Eqn. A.5 evaluates to the magnitude of the wrench.

The wrench $\mathcal{W}$ in Eqn. A.5 can be interpreted as defining a linear function on the twist $\dot{\mathbf{q}}$. This observation allows the six-dimensional space of wrenches to be interpreted as that dual to six-dimensional space of twists. Ref. [24] calls the geometric elements underlying the dual space of wrenches, *co-screws*.

Of interest is the way in which twists and wrenches transform under rigid displacement. The displacement of a twist corresponds to the adjoint action of $SE(3)$ on its Lie algebra [24].

Let $\dot{\mathbf{q}}_\mathbf{i}$ and $\dot{\mathbf{q}}_\mathbf{j}$ describe the initial and displaced coordinates of a twist under the rigid motion defined by R_k and T_k. Then

$$\dot{\mathbf{q}}_j = H_k\dot{\mathbf{q}}_i = \begin{pmatrix} R_k & 0 \\ \\ T_kR_k & R_k \end{pmatrix} \begin{pmatrix} \boldsymbol{\omega}_i \\ \\ \mathbf{v}_i \end{pmatrix} \tag{A.6}$$

where R_k is a rotational matrix describing the position vector $\mathbf{r}_\mathbf{j}$ in frame $\mathbf{i}$ satisfying $\mathbf{r}_\mathbf{i} = \mathbf{R}_\mathbf{k}\mathbf{r}_\mathbf{j}$ for pure rotation. T_k is the skew-symmetric form of $\mathbf{t}_\mathbf{k}$, satisfying $T_k\mathbf{x} = \mathbf{t}_\mathbf{k} \times \mathbf{x}$ for pure translation. Since R_k is orthogonal, the inverse

transformation matrix is

$$H_k^{-1} = \begin{pmatrix} R_k^T & 0 \\ -R_k^T T_k & R_k^T \end{pmatrix}. \tag{A.7}$$

The rule by which wrenches (and their underlying co-screws) transform under rigid motion is given by

$$\mathcal{W}_j = H_k^{-T} \mathcal{W}_i = \begin{pmatrix} R_k & T_k R_k \\ 0 & R_k \end{pmatrix} \begin{pmatrix} \boldsymbol{\tau}_i \\ \mathbf{f}_i \end{pmatrix} \tag{A.8}$$

where H_k^{-T} indicates the transposed inverse of H_k.

Where H_k is parameterized by time, the derivative of Eqn. A.6 describes how the infinitesimal motion $\dot{\mathbf{q}}_k$ corresponding to H_k acts on the twist $\dot{\mathbf{q}}_\mathbf{j}$:

$$\begin{aligned} \frac{d}{dt}\dot{\mathbf{q}}_j &= \frac{dH_k}{dt}\dot{\mathbf{q}}_i = \frac{dH_k}{dt} H_k^{-1} \dot{\mathbf{q}}_j \\ &= \begin{pmatrix} \Omega_k & 0 \\ V_k & \Omega_k \end{pmatrix} \begin{pmatrix} \boldsymbol{\omega}_j \\ \mathbf{v}_j \end{pmatrix} = \begin{pmatrix} \boldsymbol{\omega}_k \times \boldsymbol{\omega}_j \\ \mathbf{v}_k \times \boldsymbol{\omega}_j + \boldsymbol{\omega}_k \times \mathbf{v}_j \end{pmatrix} \\ &= [\dot{\mathbf{q}}_k, \dot{\mathbf{q}}_j] \end{aligned} \tag{A.9}$$

Here Ω_k is the skew-symmetric representation of the body's angular velocity $\boldsymbol{\omega}_k = (\omega_x, \omega_y, \omega_z)$, satisfying $\Omega_k \mathbf{r}_\mathbf{j} = \boldsymbol{\omega}_\mathbf{k} \times \mathbf{r}_\mathbf{j}$ and V_k is the skew-symmetric representation of the body's translational velocity $\mathbf{v_k} = (\mathbf{v_x}, \mathbf{v_y}, \mathbf{v_z})$, satisfying $V_k \mathbf{r}_\mathbf{j} = \mathbf{v_k} \times \mathbf{r_j}$.

This operation is called the *Lie bracket* of twists $\dot{\mathbf{q}}_k$ and $\dot{\mathbf{q}}_\mathbf{j}$.

The action of the twist $\dot{\mathbf{q}}_k$ on a wrench $\mathcal{W}_j$ is called the *Lie co-bracket* and is

obtained by differentiating Eqn. A.8

$$\begin{aligned}\frac{d}{dt}\mathcal{W}_j &= \frac{dH_k^{-T}}{dt} H_k^T \mathcal{W}_j \\ &= \begin{pmatrix} \Omega_k & V_k \\ 0 & \Omega_k \end{pmatrix} \begin{pmatrix} \boldsymbol{\tau}_j \\ \mathbf{f}_j \end{pmatrix} = \begin{pmatrix} \boldsymbol{\omega}_k \times \boldsymbol{\tau}_j + \mathbf{v}_k \times \mathbf{f}_j \\ \boldsymbol{\omega}_k \times \mathbf{f}_j \end{pmatrix} \\ &= \{\dot{\mathbf{q}}_k, \mathcal{W}_j\}\,.\end{aligned} \tag{A.10}$$

A.2 representation of joints, adjoint, velocities and accelerations

In rigid multi-body linkages, joints between body's can be represented by the normalized velocity screw $\mathbf{s_k}$. A revolute joint consists of a rotation axis with a position and direction. If the rotational axis' direction is given by the unit vector ϕ and its position by the position-vector $\mathbf{r}$ of any point on the axis then the resulting rotation is described by [11] as:

$$\psi = \mathbf{r} \times \phi. \tag{A.11}$$

A prismatic joint, on the other hand, consist of a translational axis with direction only. Therefor vector ϕ is zero for prismatic joints. The direction of the joint's translational axis is given by the unit vector ψ.

The 6-vector representation of the joint screw will be

$$\mathbf{s_k} = \begin{pmatrix} \phi \\ \psi \end{pmatrix}. \tag{A.12}$$

Multiple degree of freedom joints can be separated into multiple single degree of freedom joints connected by massless links.

For a description of the kinematics of a link with respect to any other linkage, the home position and joint screw adjoint, is used. The relative coordinates $\boldsymbol{\theta}_i$ describes the i-th link's joint motion with respect to the $i-1$-th link. Its home position is defined as the reference position in which $\boldsymbol{\theta}_i$ is defined to be 0. A

joint-screw in its home position is denoted $\mathbf{s}_i^0$, that is a joint screw containing the direction of motion and position information. Kinematic transforms between links can thus be described by:

$$H_i = Ad(e^{\boldsymbol{\theta}_i \mathbf{s}_i^0}) = e^{\theta_i \mathbf{S_i^0}} \tag{A.13}$$

Where $\mathbf{S^0}$ is given by:

$$\mathbf{S}^0 = \begin{pmatrix} \Phi & 0_{3\times 3} \\ \Psi & \Phi \end{pmatrix}. \tag{A.14}$$

in which Ψ is the skew symmetric form of ψ and Φ is the skew symmetric form of ϕ.

Applying the product of exponentials to Eqn. A.13 and the joint-screws in home position, $\mathbf{s}_i^0$, yields the joint-screws in the reference frame again.

$$\mathbf{s}_i = \left(\prod_{1 \preceq j \preceq i} \mathrm{Ad}\left(\boldsymbol{\theta}_j \mathbf{s}_j^0\right) \right) \mathbf{s}_i^0 = \left(\prod_{1 \preceq j \prec i} H_j \right) \mathbf{s}_i^0 \tag{A.15}$$

The products in the above expressions are over all joints that are ancestors of i, starting at the root joint.

The velocity screw of a body can be expressed in terms of joint screws and the body's relative velocity. Because $\dot{\theta}$ describes the relative velocity of the joint's degree of freedom, the body's velocity screw can be written as a summation of the products of $\dot{\theta}_\mathbf{k}$ and $\mathbf{s_k}$ of its ancestry joints.

$$\dot{\mathbf{q}}_i = \sum_{1 \preceq j \preceq i} \dot{\theta}_j \mathbf{s}_j \tag{A.16}$$

The acceleration screw is the time derivative of the velocity screw.

$$\begin{aligned} \ddot{\mathbf{q}}_i &= \sum_{1 \preceq j \preceq i} \left(\ddot{\theta}_j \mathbf{s}_j + \dot{\theta}_j \frac{d}{dt} \mathbf{s}_j \right) \\ &= \sum_{1 \preceq j \preceq i} \left(\ddot{\theta}_j \mathbf{s}_j + \dot{\theta}_j \left[\dot{\mathbf{q}}_j, \mathbf{s}_j \right] \right) \end{aligned} \tag{A.17}$$

Note that if Eqn. A.16 is substituted in Eqn. A.17 the terms $[\mathbf{s}_j, \mathbf{s}_j]$ reduce to zero.

A.3 Inertia matrix, momentum; and Newton's second law

The angular and linear momentum of a rigid body twisting about $\dot{\mathbf{q}}^T = \begin{pmatrix} \omega^T & \mathbf{v}^T \end{pmatrix}$ expressed in arbitrary frame of reference can be written

$$\begin{aligned} \mathbf{j} &= J\boldsymbol{\omega} + m\left(\mathbf{c} \times \mathbf{v}\right) \\ \mathbf{p} &= m\mathbf{v} + m\left(\boldsymbol{\omega} \times \mathbf{c}\right) \end{aligned} \tag{A.18}$$

where J is the 3×3 inertia matrix and $\mathbf{c}$ is the 3-vector giving coordinates of the mass center in the reference frame, and m is body mass. Expressed in matrix form these equations are

$$\begin{aligned} \mathcal{M} &= \begin{pmatrix} \mathbf{j} \\ \\ \mathbf{p} \end{pmatrix} = \begin{pmatrix} J & mC \\ \\ mC^T & mI_3 \end{pmatrix} \begin{pmatrix} \omega \\ \\ \mathbf{v} \end{pmatrix} \\ &= N\dot{\mathbf{q}} \end{aligned} \tag{A.19}$$

where C is the skew-symmetric form of $\mathbf{c}$ and I_3 is a 3×3 identity matrix. The six-by-six matrix matrix N is the body's *inertia matrix*.

Let N_i be the inertia matrix of a rigid body in a body-fixed frame whose motion relative to an inertial frame is given by the matrix valued function $H_k(t)$. The inertia matrix for the body in the inertial frame can be found from

$$N_k(t) = H_k\left(t\right)^{-T} N_i H_k\left(t\right)^{-1} \tag{A.20}$$

and the momentum of the body (in the inertial frame) from

$$\mathcal{M}_k(t) = N_k\left(t\right)\dot{\mathbf{q}}_k(t) = H_k^{-T}\left(t\right) N_i H_k^{-1}\left(t\right)\dot{\mathbf{q}}_k(t)$$

Differentiating this expression with respect to time gives, by Newton's second

law, the net wrench acting on the body

$$\begin{aligned}
&\mathcal{W}(t) = \frac{d\mathcal{M}_k(t)}{dt} \\
&= N_k(t)\frac{d\dot{\mathbf{q}}_k(t)}{dt} + \left(\frac{dH_k^{-T}(t)}{dt}N_i H_k^{-1}(t) + H_k^{-T}(t)N_i\frac{dH_k^{-1}(t)}{dt}\right)\dot{\mathbf{q}}_k(t) \\
&= N_k(t)\frac{d\dot{\mathbf{q}}_k(t)}{dt} + \left(\frac{dH_k^{-T}(t)}{dt}H_k^{T}(t)N_k + N_k H_k(t)\frac{dH_k^{-1}(t)}{dt}\right)\dot{\mathbf{q}}_k(t) \\
&= N_k(t)\ddot{\mathbf{q}}_k(t) + \{\dot{\mathbf{q}}_k, N_k\dot{\mathbf{q}}_k\}
\end{aligned} \tag{A.21}$$

The transition from the first to second line in the above equation makes use of Eqn. A.20 and the transition from the second to the third lines above follows from

$$\begin{aligned}
H_k(t)\frac{dH_k^{-1}(t)}{dt}\dot{\mathbf{q}}_k &= -\left[\dot{\mathbf{q}}_k,\, \dot{\mathbf{q}}_k\right] = 0 \\
\frac{dH_k^{-T}(t)}{dt}H_k^{T}(t)N_k\dot{\mathbf{q}}_k &= \{\dot{\mathbf{q}}_k, N_k\dot{\mathbf{q}}_k\}
\end{aligned}$$

Eqn. A.21 is the basis for our solution method.

References

[1] W. W. Armstrong (1979), *Recursive solution to the equations of motion of an n-link manipulator*. Proceedings of the 5th world congress on the theory of machines and mechanisms, 2, pp 1343-1346.

[2] K. S. Anderson and J.H. Critchley (2003), *Improved order-n performance algorithm for the simulation of constrained multi-rigid-body dynamic systems.* Multibody Systems Dynamics, in press.

[3] U. M. Ascher, H. Chin, L. R. Petzold and S. Reich (1995), *Stabilization fo constrained mechanical systems with DAEs and invariant manifolds.* Mechanics of structures and machines, 23, pp 135-158:

[4] V. I. Arnold (1978) *Geometrical methods of classical mechanics.* Volume 60 of Graduate Texts in Mathematics. Springer-Verlag, New York.

[5] D. S. Bae and E. J. Haug (1987) *A recursive formulation for constrained*

mechanical system dynamics: part II. Closed loop systems. Mechanics of structures and machines, 15(4), pp 481-506.

[6] R. S. Ball (1900) *The theory of screws.* Cambridge University Press, Cambridge.

[7] J. Baumgarte (1972) *Stabilization of constraints and integrals of motion in dynamical systems.* Computer methods in applied mechanics and engineering. 1 pp 1-16.

[8] N. L. Biggs (1985) *Discrete mathematics.* Oxford University Press, New York.

[9] R. W. Brockett (1993) *Robotic manipulators and the product of exponentials formula.* Proc. Symp. Math. Theory Networks and Systems. Beer Sheba, Israel, pp 120-129.

[10] R. Diestel (2000) *Graph Theory.* Electronic Edition 2000, Springer, New York.

[11] R. Featherstone (1983) *The calculation of robot dynamics using articulated-body inertias.* The international journal of robotics research. 2(1), pp 13-30.

[12] R. Featherstone and A. Fijany (1999) *A technique for analyzing constrained rigid-body systems, and its application to the constraint force algorithm.* IEEE trans on robotics and automation. 15(6), pp 1140-1144.

[13] K. H. Hunt (1978) *Kinematic geometry of mechanisms.* Clarendon Press, Oxford.

[14] J. M. Hollerbach (1980) *Manipulator dynamics and a comparative study of dynamics formulation complexity.* IEEE transactions on systems, man, and cybernetics. SMC-10(11), pp 730-736.

[15] T. R. Kane and D. A. Levinson (1983) *Multibody dynamics.* Journal of Applied Mechanics. 50, pp 1071-1078.

[16] T. R. Kane, P. W. Likins and D. A. Levinson (1983) *Spacecraft dynamics.* McGraw Hill, New York.

[17] R. W. Murray, Z. Li, and S. S. Sastry (1993) *A mathematics introduction to robotic manipulation.* CRC Press, Boca Raton.

[18] A. Muller and P. A. Maisser (2003) *Lie group formulation of kinematic and dynamics of constrained MBS and its application to analytical mechanics.* Multibody system dynamics. 9, pp 311-352.

[19] F. Reuleaux (1875) *Theortische kinematic: Grunzüge einer theorie des maschinwesens.* Vieweg, Braunschweig. Reprinted (in English) (1963) as "Kinematics of machinery" by Dover, New York.

[20] A. Reungwetwattana and S. Toyoman (2001) *An efficient dynamic formulation for multibody systems.* Multibody System Dynamics, 6, pp 267-289.

[21] G. Rodriguez (1987) *Kalman filtering, smoothing, and recursive robot arm forward and inverse dynamics.* IEEE Journal of robotics and automation, RA-3(6), pp 624-639.

[22] D. E. Rosenthal (1990) *An Order n Formulation for Robotic Systems.* The Journal of the Astronautical Sciences, 38(4), pp 511-529.

[23] B. F. Schultz (1980) *Geometrical methods of mathematical physics.* Cambridge University Press, Cambridge.

[24] J. M. Selig (1996) *Geometrical methods in robotics.* Springer-Verlag, New York.

[25] J. M. Selig, P. R. McAree (1999) *Constrained robot dynamics II: parrallel machines.* Journal of robotic systems. 16(9), pp 487-498.

[26] J. E. Shigley and J. J. Uicker, Jr (1995) *Theory of Machines and Mechanisms*, International Edition. McGraw-Hill, United States of America.

[27] J. J. Uicker (1967) *Dynamic force analysis of spatial linkages.* Journal of applied mechanics. 34, pp 418-424.

[28] J. J. Uicker (1969) *Dynamic behaviour of spatial linkages.* Journal of Engineering for industry. 91, pp 251-265.

[29] G. D. Wood (2003) *Simulating mechanical systems in Simulink with SimMechanics.* submitted for publication.

[30] M. W. Walker and D. E. Orin (1982) *Efficient dynamic computer simulation of robotic mechanisms.* Journal of dynamic systems, measurement and control. 104, pp 205-211.

[31] A. Hall (2002) *Characterizing the Operation of a large Hydraulic Excavator.* Thesis